Mathematical Biosciences and Engineering

http://www.aimspress.com/journal/mbe

MBE, 19(11): 11628–11656.
DOI: 10.3934/mbe.2022541
Received: 29 June 2022
Revised: 30 July 2022
Accepted: 07 August 2022
Published: 15 August 2022

Research article

Modeling the effect of time delay in the increment of number of hospital beds to control an infectious disease

A. K. Misra[1], Jyoti Maurya[1] and Mohammad Sajid[2,*]

[1] Department of Mathematics, Institute of Science, Banaras Hindu University, Varanasi 221005, India
[2] Department of Mechanical Engineering, College of Engineering, Qassim University, Buraydah 51452, Saudi Arabia

* **Correspondence:** Email: msajd@qu.edu.sa.

Abstract: One of the key factors to control the spread of any infectious disease is the health care facilities, especially the number of hospital beds. To assess the impact of number of hospital beds and control of an emerged infectious disease, we have formulated a mathematical model by considering population (susceptible, infected, hospitalized) and newly created hospital beds as dynamic variables. In formulating the model, we have assumed that the number of hospital beds increases proportionally to the number of infected individuals. It is shown that on a slight change in parameter values, the model enters to different kinds of bifurcations, e.g., saddle-node, transcritical (backward and forward), and Hopf bifurcation. Also, the explicit conditions for these bifurcations are obtained. We have also shown the occurrence of Bogdanov-Takens (BT) bifurcation using the Normal form. To set up a new hospital bed takes time, and so we have also analyzed our proposed model by incorporating time delay in the increment of newly created hospital beds. It is observed that the incorporation of time delay destabilizes the system, and multiple stability switches arise through Hopf-bifurcation. To validate the results of the analytical analysis, we have carried out some numerical simulations.

Keywords: hospital beds; saddle-node bifurcation; backward bifurcation; Hopf-bifurcation; BT-bifurcation; time delay

1. Introduction

Several large-scale epidemic outbreaks have occurred in recent decades, including Ebola, SARS, Zika virus, swine flu, and COVID-19, contributing to low socio-economic status and inadequate health-care access. The relative shortage of healthcare facilities, especially hospital beds, is a growing issue that can influence the subsequent care provided to the patients. Consequently, it is observed that, in order to ensure the welfare of its population, a city must have an adequate number of hospital beds.

The city incurs unnecessary costs if the number of hospital beds is too large, but there is the risk of disease outbreaks if it is too small. In 2017, there were only 5 hospital beds for every 10,000 persons (i.e., Hospital-bed-population ratio) residents in India, while this value is 22, 28, and 128 for Saudi Arabia, the United States, and Japan, respectively [1, 2]. This Hospital-bed-population ratio is very small in low-income countries [1]. According to WHO statistics, the data on in-patient bed density is one of the significant tools to assess the level of health service delivery [3]. Thus, it is more crucial to discern the impact of limited hospital beds on future dynamics of the disease and determine the number of hospital beds that can be appropriate to control infection.

There has been a considerable effort put into developing some realistic mathematical models for a better understanding of transmission dynamics of existing and emerging infectious diseases [4–19]. Such mathematical models focus on comprehending the epidemiological transmission pattern and signifying the impact of public health services to prevent the possible outbreak and transmission of the disease. For instance, Asif et al. [18] in their study, explain the transmission of influenza by using a diffusive epidemic model. Bozkurt et al. [17] study a mathematical model for COVID-19 transmission with fear in the population. In these models, the total human population has been split into different categories depending on the status of individuals concerning infection. The simplest epidemic models to study and to tackle with are SIR and SIS type models [14, 19]. In these models total human population is either subcategorized into two classes (i.e., susceptible (S) and infected (I)) or three classes (i.e., susceptible(I) and recovered (R)). Umar et al. [19] establish an SIR epidemic model for dengue fever and study it using the artificial neural networks along with the Levenberg-Marquardt backpropagation technique, i.e., ANNs-LMB. Apart from this, only a few mathematical modelers have incorporated the hospital beds and other medical resources in their proposed model to address the impact of healthcare resources on the control of disease outbreaks [20–38]. In this regard, Karnon et al. [27] describe several case studies that illustrate the role of mathematical modeling in improving healthcare delivery with various mathematical techniques. In each case, they found that mathematical research has been able to add to the expertise of the clinicians and policymakers. Further, considering the WHO hospital-beds-population ratio (HBPR) rationale, Shan and Zhu [32] have studied an SIR epidemic model by considering standard incidence rate and nonlinear recovery rate that depends on the number of hospital beds. Also, Saha and Ghosh [31] consider a deterministic model with logistic growth in susceptible population and a nonlinear treatment rate with limited hospital beds and found that the dynamical behavior of the proposed model not only depends on the basic reproduction number but also affected by the number of hospital beds, vaccination, and other medical resources. Moreover, Njankou and Nyabadza [24] have presented an epidemiological model to investigate the future course of Ebola virus disease when hospital beds are limited. Their mathematical findings suggest that the supply of hospital beds in Ebola treatment units has a decisive role in reducing the number of Ebola patients. To analyze the impact of hospital beds and spatial heterogeneity, Zhang et al. [35] has proposed a diffusive SIS model in the heterogeneous environment for prevention and control of an infectious disease. During the COVID-19 pandemic in 2021, Booton et al. [22] established a regional mathematical model to estimate the number of infected individuals, death caused by the infection, and the required number of hospital beds (acute and intensive care). Also, Area et al. [23] developed a compartmental mathematical mode model for COVID-19 to predict the number of beds required in intensive care unit. Their study is helpful to manage the number of beds in intensive care unit.

Further, Misra and Jyoti [29] have discussed a mathematical model with a limited number of regular and temporary hospital beds. In their study, they assumed that a fixed number of temporary hospital beds are introduced during an epidemic outbreak to reduce the surge in hospitals. From this, it is found that the introduction of temporary hospital beds can lessen the number of infected individuals and the number of deaths caused by the infection. However, the medical resources used to control the disease are always limited, and the policies that intervene vary depending upon the number of infected individuals [30]. Thus, the common wisdom is that the number of hospital beds should be increased with the increasing number of infected population.

From the above, it is shown that maintaining enough beds in the hospital is decisive to restrain the spread of infection in the population. Motivated from the prior discussion, in this paper, we study the disease dynamics when the number of hospital beds is being incremented in proportion to the increasing number of infected individuals. Also, the process to construct new hospital beds require a lot of effort, time, and money, which may lead to some time lag between the construction of new hospital beds and the current data of infected individuals. Therefore, we also introduce a delay in the increment of new hospital beds to intervene in a more realistic situation.

2. The mathematical model

It is a well-established fact that new beds are created in hospitals every day, and this has considerable implications for future patient dynamics of infectious diseases. Thus, to assess this effect on a disease outbreak, we have classified the total human population $N(t)$ into three categories: $S(t)$, $I(t)$, and $H(t)$ sequentially represent the population of susceptible, infected, and hospitalized at time t. The allocation of hospital beds in any hospital depends on the demand. Thus, we assume that H_b is the number of newly created hospital beds that are increased with an increasing number of infected population at time t that are created at a rate ϕ. We also consider that some hospital beds are not functioning properly and thus decreased with a rate ϕ_0.

The term $(H_a + H_b - H)$ (here $H \leq H_a + H_b$) in model system (2.1) represents number of available hospital beds at any instant of time t, where H_a is the total number of pre-existing hospital beds. The basic notion of the proposed model is that healthy people come in contact with infected individuals, contract infection, and become infective. Here, we assume that the contact rate of susceptible population with infected individuals is proportional to the total population size N; therefore, we consider the simple mass action incidence rate βSI for the proposed model. This term βSI, represents the transmission of individuals from the susceptible class to the infected class at time t, where β is the average number of adequate contacts per unit time with infected individuals (also called transmission rate). The constants d, α, ν, and ν_1 sequentially represent the natural mortality, disease-induced mortality, self-recovery and hospital recovery rates. The parameters A and k_1 are immigration and hospital bed occupancy rates, respectively. We assume that some hospitalized population may die in the hospital because of infection, thus experience some extra mortality due to the emerged infectious disease with proportionality constant θ.

From the above consideration, the rate of change of each class of human population (i.e., susceptible, infected, and hospitalized) and newly created hospital beds is given by the following system:

$$\begin{cases} \dfrac{dS}{dt} = A - \beta S I - dS + \nu I + \nu_1 H, \\ \dfrac{dI}{dt} = \beta S I - (\nu + \alpha + d)I - k_1(H_a + H_b - H)I, \\ \dfrac{dH}{dt} = k_1(H_a + H_b - H)I - (d + \theta\alpha + \nu_1)H, \\ \dfrac{dH_b}{dt} = \phi I - \phi_0 H_b. \end{cases} \tag{2.1}$$

Here, $S(0) = S_0 > 0$, $I(0) = I_0 \geq 0$, $H(0) = H_0 \geq 0$ and $H_b(0) = H_{b_0} \geq 0$.

3. Basic properties

3.1. Model equilibria

The model system (2.1) always has equilibrium $E_0\left(\dfrac{A}{d}, 0, 0, 0\right)$ at which the infected population is zero (i.e., $I = 0$). Thus, the basic reproduction number is obtained as

$$R_0 = \frac{\beta A}{d(\nu + \alpha + d + k_1 H_a)}.$$

For $I \neq 0$, the components S, I, H of any endemic equilibrium satisfies,

$$S(I) = \frac{1}{\beta}\left\{(\nu + \alpha + d + k_1 H_a) + \frac{k_1\phi}{\phi_0}I - \frac{k_1^2\left(H_a + \frac{\phi}{\phi_0}I\right)I}{(d + \theta\alpha + \nu_1 + k_1 I)}\right\},\ H(I) = \frac{k_1\left(H_a + \frac{\phi}{\phi_0}I\right)I}{(d + \theta\alpha + \nu_1 + k_1 I)},\ H_b(I) = \frac{\phi}{\phi_0}I,$$

and the component I must be the real positive solution(s) of the following quadratic polynomial:

$$\mathcal{F}(I) = \mathcal{A}_1 I^2 + \mathcal{A}_2 I - \mathcal{A}_3, \tag{3.1}$$

where

$$\begin{aligned} \mathcal{A}_1 &= \beta k_1\Big\{\phi_0(\alpha + d) + \phi(d + \theta\alpha)\Big\}, \\ \mathcal{A}_2 &= \beta\phi_0\Big\{(\alpha + d)(d + \theta\alpha + \nu_1) + k_1 H_a(d + \theta\alpha) - k_1 A\Big\} + k_1 d\Big\{\phi_0(\nu + \alpha + d) + \phi(d + \theta\alpha + \nu_1)\Big\}, \\ \mathcal{A}_3 &= \phi_0 d(R_0 - 1)(\nu + \alpha + d + k_1 H_a)(d + \theta\alpha + \nu_1). \end{aligned}$$

We set, $\mathcal{D}_0 = \mathcal{A}_2^2 + 4\beta\phi_0 k_1 d(R_0 - 1)(\nu + \alpha + d + k_1 H_a)(d + \theta\alpha + \nu_1)\Big\{\phi_0(\alpha + d) + \phi(d + \theta\alpha)\Big\}$.
Further, for $R_0 > 1$ the equation $\mathcal{F}(I) = 0$ always has a real positive root and has two real positive roots if and only if $R_0 < 1$, $\mathcal{A}_2 < 0$, and $\mathcal{D}_0 > 0$, that can be written as:

$$I_1^* = \frac{-\mathcal{A}_2 + \sqrt{\mathcal{D}_0}}{2\mathcal{A}_1},\ \text{and}\ I_2^* = \frac{-\mathcal{A}_2 - \sqrt{\mathcal{D}_0}}{2\mathcal{A}_1},\ \text{here}\ I_1^* > I_2^*.$$

Moreover, for $\mathcal{A}_2 < 0$ and $\mathcal{D}_0 = 0$, we obtained a threshold value R_c of R_0, that can be written as

$$R_c = 1 - \frac{\mathcal{A}_2^2}{4\mathcal{A}_1\phi_0 d(\nu + \alpha + d + k_1 H_a)(d + \theta\alpha + \nu_1)}.$$

Therefore, the results regarding existence of equilibrium of model system (2.1) are concluded in the theorem below:

Theorem 1. *The model system* (2.1) *has*

(i) A disease-free equilibrium $E_0\left(\frac{A}{d}, 0, 0, 0\right)$*, which always exists.*

(ii) A unique endemic equilibrium E_1^**, it exists whenever* $R_0 > 1$*.*

(iii) A unique endemic equilibrium E_1^**, it exists when* $R_0 = 1$*, provided* $\mathcal{A}_2 < 0$*, otherwise no endemic equilibrium exists.*

(iv) Two endemic equilibria E_1^* *and* E_2^**, exist whenever* $R_0 < 1$*, provided* $\mathcal{A}_2 < 0$ *and* $\mathcal{D}_0 > 0$*; otherwise no endemic equilibrium exists. These two equilibria (*E_1^* *and* E_2^**) collide and unite into a unique endemic equilibrium* E_3^* *when* $\mathcal{D}_0 = 0$ *and* $\mathcal{A}_2 < 0$ *(or equivalently* $R_0 = R_c$*).*

3.2. Local stability analysis

At equilibrium E_0 the Jacobian matrix for model system (2.1) is given by

$$J_0 = \begin{bmatrix} -d & -\left(\frac{\beta A}{d} - \nu\right) & \nu_1 & 0 \\ 0 & (R_0 - 1)(\nu + \alpha + d + k_1 H_a) & 0 & 0 \\ 0 & k_1 H_a & -(d + \theta\alpha + \nu_1) & 0 \\ 0 & \phi & 0 & -\phi_0 \end{bmatrix}.$$

The above matrix yield four eigenvalues (i.e., $-d$, $-(d + \theta\alpha + \nu_1)$, $-\phi_0$, and $(R_0 - 1)(\nu + \alpha + d + k_1 H_a)$), from which three are always negative and $(R_0 - 1)(\nu + \alpha + d + k_1 H_a)$ depends on the value of R_0. Thus, results regarding nature of equilibrium E_0 are compiled in the theorem below:

Theorem 2. *The equilibrium* E_0 *, is locally asymptotically stable until* $R_0 < 1$*, as* R_0 *exceed unity, it becomes unstable.*

Now, the Jacobian matrix for model system (2.1), calculated at any endemic equilibrium is written as

$$J^* = \begin{bmatrix} -(\beta I^* + d) & -(\beta S^* - \nu) & \nu_1 & 0 \\ \beta I^* & 0 & k_1 I^* & -k_1 I^* \\ 0 & k_1(H_a + H_b^* - H^*) & -(d + \theta\alpha + \nu_1 + k_1 I^*) & k_1 I^* \\ 0 & \phi & 0 & -\phi_0 \end{bmatrix}.$$

One can easily verify that the eigenvalues of the above matrix J^* are the solutions of the equation:

$$\xi^4 + \mathcal{B}_1\xi^3 + \mathcal{B}_2\xi^2 + \mathcal{B}_3\xi + \mathcal{B}_4 = 0, \tag{3.2}$$

here

$$\mathcal{B}_1 = 2d + \theta\alpha + \nu_1 + \phi_0 + k_1 I^* + \beta I^*,$$

$$\mathcal{B}_2 = \phi_0(d + \theta\alpha + \nu_1 + k_1 I^*) + (\beta I^* + d)(d + \theta\alpha + \nu_1 + \phi_0 + k_1 I^*) + \beta I^*(\beta S^* - \nu) + k_1\phi I^* - k_1^2 I^*(H_a + H_b^* - H^*),$$

$$\mathcal{B}_3 = \phi_0(\beta I^* + d)(d + \theta\alpha + \nu_1 + k_1 I^*) + \beta I^*(\beta S^* - \nu)(d + \theta\alpha + \nu_1 + \phi_0 + k_1 I^*) + k_1\phi I^*(2d + \theta\alpha + \nu_1 + k_1 I^* + \beta I^*)$$
$$- k_1^2 I^*[\phi_0(H_a + H_b^* - H^*) + \phi I^*] - k_1 I^*(H_a + H_b^* - H^*)[k_1(\beta I^* + d) + \beta\nu_1],$$

$$\mathcal{B}_4 = \beta\phi_0 I^*(\beta S^* - \nu)(d + \theta\alpha + \nu_1 + k_1 I^*) + k_1\phi I^*(\beta I^* + d)(d + \theta\alpha + \nu_1 + k_1 I^*)$$
$$- k_1 I^*[k_1(\beta I^* + d) + \beta\nu_1][\phi_0(H_a + H_b^* - H^*) + \phi I^*].$$

One can see that $\mathcal{B}_1$ is always positive and using Eq (3.1), we can rewrite $\mathcal{B}_4$ as

$$\mathcal{B}_4 = \frac{I^*}{(d + \theta\alpha + \nu_1 + k_1 I^*)}[k_1(\mathcal{A}_1 I^{*2} + \mathcal{A}_3) + (2\mathcal{A}_1 I^* + \mathcal{A}_2)(d + \theta\alpha + \nu_1)].$$

Therefore, based on the above expression, we can say that $I^* = I_1^*$ gives, $\mathcal{B}_4 > 0$. Further, $I^* = I_2^*$ gives $\mathcal{B}_4 < 0$ when $R_0 < 1$. Therefore, using the Routh-Hurwitz criterion, we can state that the equilibrium E_1^* is locally asymptotically stable iff

$$\mathcal{B}_3 > 0 \text{ and } \mathcal{B}_3(\mathcal{B}_1\mathcal{B}_2 - \mathcal{B}_3) - \mathcal{B}_1^2\mathcal{B}_4 > 0, \tag{3.3}$$

whereas E_2^* is unstable whenever exists. Thus, the results regarding local stability behavior of endemic equilibria are compiled in theorem below:

Theorem 3. *If system* (2.1)*, has simply a unique endemic equilibrium E_1^*, then it is locally asymptotically stable iff $\mathcal{B}_3 > 0$ and $\mathcal{B}_3(\mathcal{B}_1\mathcal{B}_2 - \mathcal{B}_3) - \mathcal{B}_1^2\mathcal{B}_4 > 0$. If there exists exactly two endemic equilibria, then the endemic equilibrium with high endemicity (i.e., E_1^*) is locally asymptotically stable iff $\mathcal{B}_3 > 0$ and $\mathcal{B}_3(\mathcal{B}_1\mathcal{B}_2 - \mathcal{B}_3) - \mathcal{B}_1^2\mathcal{B}_4 > 0$, whereas the equilibrium with low endemicity (i.e., E_2^*) is unstable, whenever exists.*

4. Bifurcation analysis

4.1. Transcritical bifurcation

$$J_0(\beta^*) = \begin{bmatrix} -d & -\left(\frac{\beta^* A}{d} - \nu\right) & \nu_1 & 0 \\ 0 & (R_0 - 1)(\nu + \alpha + d + k_1 H_a) & 0 & 0 \\ 0 & k_1 H_a & -(d + \theta\alpha + \nu_1) & 0 \\ 0 & \phi & 0 & -\phi_0 \end{bmatrix}.$$

Thus, the matrix $J_0(\beta^*)$ simply has one zero eigenvalue at $R_0 = 1$, and the rest three eigenvalues (i.e., $-d$, $-(d + \theta\alpha + \nu_1)$, and $-\phi_0$) are negative. Therefore, to identify the direction of transcritical bifurcation, we first obtain the right eigenvector ($\tilde{U} = (\tilde{u}_1, \tilde{u}_2, \tilde{u}_3, \tilde{u}_4)^T$) and left eigenvector ($\tilde{V} = (\tilde{v}_1, \tilde{v}_2, \tilde{v}_3, \tilde{v}_4)$) of the matrix $J_0(\beta^*)$ corresponding to the zero eigenvalue, which are given as follows:

$$\tilde{U} = \begin{bmatrix} -\left(\frac{\beta^* A}{d} - \nu\right)(d + \theta\alpha + \nu_1) + \nu_1 k_1 H_a \\ d(d + \theta\alpha + \nu_1) \\ d k_1 H_a \\ \frac{\phi}{\phi_0} d(d + \theta\alpha + \nu_1) \end{bmatrix}, \tilde{V}^T = \begin{bmatrix} 0 \\ 1 \\ 0 \\ 0 \end{bmatrix}.$$

Now, the coefficients $\tilde{a}$ and $\tilde{b}$, in [39] for model system (2.1) can be calculated as $\tilde{a} = \sum_{i,j,k=1}^{4} \tilde{v}_k \tilde{u}_i \tilde{u}_k \frac{\partial^2 \tilde{f}_k}{\partial \tilde{x}_i \partial \tilde{x}_j}(E_0, \beta^*)$, and $\tilde{b} = \sum_{i,k=1}^{4} \tilde{v}_k \tilde{u}_i \frac{\partial^2 \tilde{f}_k}{\partial \tilde{x}_i \partial \beta}(E_0, \beta^*)$ (here f_k, $k = 1, \ldots, 4$ are right hand side of $\frac{d\tilde{x}_i}{dt}$, $i = 1, \ldots, 4$ of model system (2.1)). Thus, we have

$$\tilde{a} = 2d(d + \theta\alpha + \nu_1)\left\{ -\left[\beta^*\left(\frac{\beta^* A}{d} - \nu\right) + k_1 d\frac{\phi}{\phi_0}\right](d + \theta\alpha + \nu_1) + k_1 H_a(k_1 d + \beta^* \nu_1)\right\}, \text{ and } \tilde{b} = A(d + \theta\alpha + \nu_1).$$

From the above expression, it is clear that $\tilde{b}$ is always greater than zero, thus applying the condition (*i*) and (*iv*) of Theorem 4.1 of [39]. Therefore, the following theorem emerges:

Theorem 4. *The direction of transcritical bifurcation for model system* (2.1) *is*

(i) backward if $\left[\beta^*\left(\frac{\beta^* A}{d} - \nu\right) + k_1 d\frac{\phi}{\phi_0}\right] < k_1 H_a\left(\frac{k_1 d + \beta^* \nu_1}{d + \theta\alpha + \nu_1}\right)$, *and*

(ii) forward if $\left[\beta^*\left(\frac{\beta^* A}{d} - \nu\right) + k_1 d\frac{\phi}{\phi_0}\right] > k_1 H_a\left(\frac{k_1 d + \beta^* \nu_1}{d + \theta\alpha + \nu_1}\right)$.

4.2. Saddle-node bifurcation

Here, we demonstrate the saddle-node bifurcation phenomenon through the application of Sotomayor's theorem. Keeping this aim in mind, we first select β as a bifurcation parameter. According to Theorem 1 system (2.1) possess exactly one endemic equilibrium E_3^* at $R_0 = R_c$ (or $\beta = \beta_c$) at which the Jacobian matrix $J^*(E_3^*, \beta_c)$ has a simple zero eigenvalue. Let $\widehat{U}^T = (\widehat{u_1}, \widehat{u_2}, \widehat{u_3}, \widehat{u_4})$ and $\widehat{V} = (\widehat{v_1}, \widehat{v_2}, \widehat{v_3}, \widehat{v_4})$ are respectively, the right and left eigenvector of matrix $J^*(E_3^*, \beta_c)$, with respect to the zero eigenvalue. Thus, we have

$$\widehat{U} = \begin{bmatrix} -k_1^2\phi_0(H_a + H_{b_3}^* - H_3^*) + k_1\phi(d + \theta\alpha + \nu_1) \\ \beta_c\phi_0(d + \theta\alpha + \nu_1 + k_1 I_3^*) \\ \beta_c k_1[\phi_0(H_a + H_{b_3}^* - H_3^*) + \phi I_3^*] \\ \beta_c\phi(d + \theta\alpha + \nu_1 + k_1 I_3^*) \end{bmatrix}, \text{ and } \widehat{V}^T = \begin{bmatrix} \beta_c\phi_0 I_3^*(d + \theta\alpha + \nu_1 + k_1 I_3^*) \\ \phi_0(\beta_c I_3^* + d)(d + \theta\alpha + \nu_1 + k_1 I_3^*) \\ \phi_0 I_3^*[\beta_c\nu_1 + k_1(\beta_c I_3^* + d)] \\ -k_1 I_3^*[\beta_c I_3^*(d + \theta\alpha) + d(d + \theta\alpha + \nu_1)] \end{bmatrix}$$

Now, we consider that $\widehat{\mathcal{F}} = (\widehat{f_1}, \widehat{f_2}, \widehat{f_3}, \widehat{f_4})$, here $\widehat{f_1}$, $\widehat{f_2}$, $\widehat{f_3}$, and $\widehat{f_4}$ are respectively, the right hand side of dS/dt, dI/dt, dH/dt, and dH_b/dt in model system (2.1). Thus, we have

$$\widehat{\mathscr{B}}_1 = \widehat{V}.\frac{\partial \mathcal{F}}{\partial \beta}\bigg|_{\left(E_3^*, \beta_c(\text{or } R_c)\right)} = \phi_0 d(d + \theta\alpha + \nu_1 + k_1 I_3^*) S_3^* I_3^* > 0, \text{ and} \tag{4.1}$$

$$\begin{aligned} \widehat{\mathscr{B}}_2 &= \widehat{V}.[D^2_{(S,I,H,H_b)}\widehat{\mathcal{F}}(\widehat{U}, \widehat{U})]\Big|_{\left(E_3^*, \beta_c(\text{or } R_c)\right)} \\ &= -2\beta_c^2\phi_0^3 k_1(d + \theta\alpha + \nu_a + k_1 I_3^*)(d + \theta\alpha + \nu_1)(H_{b_3}^* - H_3^*)\Big[\beta_c(d + \theta\alpha) - k_1 d\Big] \neq 0, \\ &\quad \text{provided } H_{b_3}^* \neq H_3^*, \text{ and } k_1 \neq \frac{\beta_c(d + \theta\alpha)}{d}. \end{aligned} \tag{4.2}$$

From Eqs (4.1) and (4.2), Sotomayor's theorem demonstrates that saddle-node bifurcation exists at $\beta = \beta_c$ (or equivalently $R_0 = R_c$). Therefore, the resulting theorem is as follows:

Theorem 5. *The equilibrium E_3^* is saddle in nature, iff $H_{b3}^* \neq H_3^*$, and $k_1 \neq \dfrac{\beta_c(d+\theta\alpha)}{d}$.*

4.3. Hopf-bifurcation

We select transmission rate β as a bifurcation parameter to establish existence of Hopf-bifurcation at equilibrium E_1^*. As a result, we can write each coefficient of the characteristic Eq (3.2) as a function of β, which gives

$$\xi^4 + \mathcal{B}_1(\beta)\xi^3 + \mathcal{B}_2(\beta)\xi^2 + \mathcal{B}_3(\beta)\xi + \mathcal{B}_4(\beta) = 0. \tag{4.3}$$

We consider that, $\beta = \beta_r$ gives $\mathcal{B}_i(\beta_r) > 0$ $(i = 3, 4)$, and $\mathcal{B}_3(\beta_r)\Big(\mathcal{B}_1(\beta_r)\mathcal{B}_2(\beta_r) - \mathcal{B}_3(\beta_r)\Big) - \mathcal{B}_1^2(\beta_r)\mathcal{B}_4(\beta_r) = 0$. Therefore, the Eq (3.2) can be written as

$$\left(\xi^2 + \frac{\mathcal{B}_3}{\mathcal{B}_1}\right)\left(\xi^2 + \mathcal{B}_1\xi + \frac{\mathcal{B}_1\mathcal{B}_4}{\mathcal{B}_3}\right) = 0. \tag{4.4}$$

The Eq (4.4) has four roots ξ_i $(i = 1, \ldots, 4)$, with a pair of purely imaginary roots $\xi_{1,2} = \pm i\psi_0$, where $\psi_0 = (\mathcal{B}_3/\mathcal{B}_1)^{1/2}$. The nature of remaining two roots (i.e., ξ_3 and ξ_4) can be identified with help of following set of equations:

$$\begin{cases} \xi_3 + \xi_4 = -\mathcal{B}_1, \\ \psi_0^2 + \xi_3\xi_4 = \mathcal{B}_2, \\ \psi_0^2(\xi_3 + \xi_4) = -\mathcal{B}_3, \\ \psi_0^2\xi_3\xi_4 = \mathcal{B}_4. \end{cases}$$

Therefore, we can say that ξ_3 and ξ_4 are always lies in the left half plane. Further, we choose any point in the $\epsilon-$neighborhood of β for which $\xi_{1,2} = \omega(\beta) \pm i\kappa(\beta)$. When we substitute this in Eq (4.3) and writing separately real and imaginary components, we obtain

$$\omega^4 + \mathcal{B}_1\omega^3 + \mathcal{B}_2\omega^2 + \mathcal{B}_3\omega + \mathcal{B}_4 + \kappa^4 - 6\omega^2\kappa^2 - 3\mathcal{B}_1\omega\kappa^2 - \mathcal{B}_2\kappa^2 = 0, \tag{4.5}$$

and

$$4\omega\kappa(\omega^2 - \kappa^2) - \mathcal{B}_1\kappa^3 + 3\mathcal{B}_1\omega^2\kappa + 2\mathcal{B}_2\omega\kappa + \mathcal{B}_3\kappa = 0. \tag{4.6}$$

As we know that $\kappa(\beta) \neq 0$, therefore from Eq (4.6), we have $-(4\omega + \mathcal{B}_1)\kappa^2 + 4\omega^3 + 3\mathcal{B}_1\omega^2 + 2\mathcal{B}_2\omega + \mathcal{B}_3 = 0$. Substituting this in Eq (4.5), we obtain

$$\left[\frac{d\omega}{d\beta}\right]_{\beta=\beta_r} = \left[\frac{\frac{d}{d\beta}\Big(\mathcal{B}_1\mathcal{B}_2\mathcal{B}_3 - \mathcal{B}_3^2 - \mathcal{B}_1^2\mathcal{B}_4\Big)}{-2\mathcal{B}_1\Big(\mathcal{B}_1\mathcal{B}_3 + (2\mathcal{B}_3/\mathcal{B}_1 - \mathcal{B}_2)^2\Big)}\right]_{\beta=\beta_r} \neq 0,$$

$$\text{provided } \frac{d}{d\beta}\Big(\mathcal{B}_1\mathcal{B}_2\mathcal{B}_3 - \mathcal{B}_3^2 - \mathcal{B}_1^2\mathcal{B}_4\Big) \neq 0.$$

Thus, the transversality condition holds if

$$\left[\frac{d}{d\beta}\Big(\mathcal{B}_1\mathcal{B}_2\mathcal{B}_3 - \mathcal{B}_3^2 - \mathcal{B}_1^2\mathcal{B}_4\Big)\right]_{\beta=\beta_r} \neq 0.$$

This leads us to the theorem below:

Theorem 6. *The model system* (2.1) *exhibits Hopf-bifurcation around the equilibrium E_1^* if there exists $\beta = \beta_r$, for which*

$$\left.\begin{aligned} &(i)\ \ \mathcal{B}_i > 0\ \ (\text{for } i = 3, 4),\\ &(ii)\ \ \mathcal{B}_3(\beta_r)\Big(\mathcal{B}_1(\beta_r)\mathcal{B}_2(\beta_r) - \mathcal{B}_3(\beta_r)\Big) - \mathcal{B}_1^2(\beta_r)\mathcal{B}_4(\beta_r) = 0,\\ &(iii)\ \ \left[\frac{d}{d\beta}\Big(\mathcal{B}_1\mathcal{B}_2\mathcal{B}_3 - \mathcal{B}_3^2 - \mathcal{B}_1^2\mathcal{B}_4\Big)\right]_{\beta=\beta_r} \neq 0. \end{aligned}\right\}$$

4.4. Bogdanov-Takens bifurcation

Here, we show the existence of BT-bifurcation of co-dimension 2 in a small neighborhood of endemic equilibrium E_3^*. Now, one can easily note that $\mathcal{B}_4\big|_{R_0=R_c} = 0$, therefore if we assume $\mathcal{B}_3\big|_{R_0=R_c} = 0$, and $\mathcal{B}_2\big|_{R_0=R_c} > 0$, Equation (3.2) produces a simple zero eigenvalue with algebraic multiplicity 2, and two eigenvalues (i.e., σ_3 and σ_4) are negative or contain negative real parts.
Now, we shift the endemic equilibrium E_3^* to origin using the transformation $\tilde{y}_1 = S - S_3^*$, $\tilde{x}_2 = I - I_3^*$, $\tilde{y}_3 = H - H_3^*$ and $\tilde{y}_4 = H_b - H_{b3}{}^*$. Thus, the model system (4.6) can be written as

$$\begin{bmatrix} \tilde{y}_1 \\ \tilde{y}_2 \\ \tilde{y}_3 \\ \tilde{y}_4 \end{bmatrix}' = \begin{bmatrix} -(\beta I_3^* + d) & -(\beta S_3^* - \nu) & \nu_1 & 0 \\ \beta I_3^* & 0 & k_1 I_3^* & -k_1 I_3^* \\ 0 & k_1(H_a + H_{b3}{}^* - H_3^*) & -(d + \theta\alpha + \nu_1 + k_1 I_3^*) & k_1 I_3^* \\ 0 & \phi & 0 & -\phi_0 \end{bmatrix} \begin{bmatrix} \tilde{y}_1 \\ \tilde{y}_2 \\ \tilde{y}_3 \\ \tilde{y}_4 \end{bmatrix} + \begin{bmatrix} g_1 \\ g_2 \\ g_3 \\ 0 \end{bmatrix} \tag{4.7}$$

where

$$g_1 = -\beta\tilde{y}_1\tilde{y}_2,\ g_2 = \beta\tilde{y}_1\tilde{y}_2 - k_1(\tilde{y}_4 - \tilde{y}_3)\tilde{y}_2,\ g_3 = k_1(\tilde{y}_4 - \tilde{y}_3)\tilde{y}_2.$$

Now, the generalized eigenvector corresponding to eigenvalues $\sigma_{1,2} = 0$ are $\mathcal{V}_1 = [v_{11}, v_{21}, v_{31}, v_{41}]^T$, and $\mathcal{V}_2 = [v_{12}, v_{22}, v_{32}, 0]^T$. Here,

$v_{11} = k_1[\phi(d + \theta\alpha + \nu_1) - k_1\phi_0(H_a + H_{b3}{}^* - H_3^*)]$, $v_{21} = \beta\phi_0(d + \theta\alpha + \nu_1 + k_1 I_3^*)$, $v_{31} = \beta k_1[\phi_0(H_a + H_{b3}{}^* - H_3^*) + \phi I_3^*]$
$v_{41} = \beta\phi(d + \theta\alpha + \nu_1 + k_1 I_3^*)$, $v_{12} = \phi(d + \theta\alpha + \nu_1 + k - 1I_3^*)v_{21} - k_1 I_3^*[-\phi v_{31} + k_1(H_a + H_{b3}{}^* - H_3^*)v_{41}]$,
$v_{22} = \beta I_3^*(d + \theta\alpha + \nu_1 + k_1 I_3^*)v_{41}$, $v_{32} = \beta I_3^*[-\phi v_{31} + k_1(H_a + H_{b3}{}^* - H_3^*)v_{41}]$.

Also, $\mathcal{V}_3 = [v_{13}, v_{23}, v_{33}, v_{43}]^T$, and $\mathcal{V}_4 = [v_{14}, v_{24}, v_{34}, v_{44}]^T$ are the eigenvectors corresponding to σ_3 and σ_4, respectively, where

$$
\begin{aligned}
&v_{13} = \sigma_3(\phi_0 + \sigma_3)(d + \theta\alpha + \nu_1 + k_1 I_3^* + \sigma_3) - k_1^2 I_3^*(H_a + H_{b3}{}^* - H_3^*)(\phi_0 + \sigma_3) + k_1\phi I_3^*(d + \theta\alpha + \nu_1 + \sigma_3),\\
&v_{23} = \beta I_3^*(\phi_0 + \sigma_3)(d + \theta\alpha + \nu_1 + k_1 I_3^* + \sigma_3),\ v_{33} = \beta k_1 I_3^*[(H_a + H_{b3}{}^* - H_3^*)(\phi_0 + \sigma_3) + \phi I_3^*]\\
&v_{43} = \beta\phi I_3^*(d + \theta\alpha + \nu_1 + k_1 I_3^* + \sigma_3),\\
&v_{14} = \sigma_4(\phi_0 + \sigma_4)(d + \theta\alpha + \nu_1 + k_1 I_3^* + \sigma_4) - k_1^2 I_3^*(H_a + H_{b3}{}^* - H_3^*)(\phi_0 + \sigma_4) + k_1\phi I_3^*(d + \theta\alpha + \nu_1 + \sigma_4),\\
&v_{24} = \beta I_3^*(\phi_0 + \sigma_4)(d + \theta\alpha + \nu_1 + k_1 I_3^* + \sigma_4),\ v_{34} = \beta k_1 I_3^*[(H_a + H_{b3}{}^* - H_3^*)(\phi_0 + \sigma_4) + \phi I_3^*]\\
&v_{44} = \beta\phi I_3^*(d + \theta\alpha + \nu_1 + k_1 I_3^* + \sigma_4).
\end{aligned}
$$

Let $\mathcal{M} = [\mathcal{V}_1, \mathcal{V}_2, \mathcal{V}_3, \mathcal{V}_4]$. Then under the transformation $\mathcal{Y} = \mathcal{M}\mathcal{X}$, where $\mathcal{X} = [\tilde{x}_1, \tilde{x}_2, \tilde{x}_3, \tilde{x}_4]^T$, $\mathcal{Y} = [\tilde{y}_1, \tilde{y}_2, \tilde{y}_3, \tilde{y}_4]$, and $\mathcal{M}^{-1}$ (inverse of the matrix $\mathcal{M}$) is

$$
\mathcal{M}^{-1} = \begin{bmatrix} \tilde{n}_{11} & \tilde{n}_{12} & \tilde{n}_{13} & \tilde{n}_{14} \\ \tilde{n}_{21} & \tilde{n}_{22} & \tilde{n}_{23} & \tilde{n}_{24} \\ \tilde{n}_{31} & \tilde{n}_{32} & \tilde{n}_{33} & \tilde{n}_{34} \\ \tilde{n}_{41} & \tilde{n}_{42} & \tilde{n}_{43} & \tilde{n}_{44} \end{bmatrix}
$$

the system (4.7) expressed as:

$$
\begin{cases}
\tilde{x}_1' = \tilde{x}_2 + P_{20}\tilde{x}_1^2 + P_{11}\tilde{x}_1\tilde{x}_2 + P_{02}\tilde{x}_2^2 + O\Big(|\tilde{x}_1, \tilde{x}_2, \tilde{x}_3, \tilde{x}_4|^2\Big),\\
\tilde{x}_2' = Q_{20}\tilde{x}_1^2 + Q_{11}\tilde{x}_1\tilde{x}_2 + Q_{02}\tilde{x}_2^2 + O\Big(|\tilde{x}_1, \tilde{x}_2, \tilde{x}_3, \tilde{x}_4|^2\Big),\\
\tilde{x}_3' = \sigma_3\tilde{x}_3 + O\Big(|\tilde{x}_1, \tilde{x}_2, \tilde{x}_3, \tilde{x}_4|^2\Big),\\
\tilde{x}_4' = \sigma_4\tilde{x}_4 + O\Big(|\tilde{x}_1, \tilde{x}_2, \tilde{x}_3, \tilde{x}_4|^2\Big).
\end{cases} \tag{4.8}
$$

Here,

$$
\begin{aligned}
P_{20} &= -\beta\tilde{n}_{11}v_{11}v_{21} + \tilde{n}_{12}[\beta v_{11}v_{12} - k_1 v_{21}(v_{41} - v_{31})] + k_1\tilde{n}_{13}v_{21}(v_{41} - v_{31}),\\
Q_{20} &= -\beta\tilde{n}_{21}v_{11}v_{21} + \tilde{n}_{22}[\beta v_{11}v_{12} - k_1 v_{21}(v_{41} - v_{31})] + k_1\tilde{n}_{23}v_{21}(v_{41} - v_{31}),\\
Q_{11} &= -\beta\tilde{n}_{12}[v_{11}v_{22} + v_{21}v_{12}] + \tilde{n}_{22}\Big\{\beta(v_{11}v_{22} + v_{21}v_{12}) - k_1[(v_{41} - v_{31})v_{22} - v_{32}v_{21}]\Big\}\\
&\quad + k_1\tilde{n}_{23}[(v_{41} - v_{31})v_{22} - v_{32}v_{21}].
\end{aligned}
$$

Here, we omit the coefficients of other quadratic terms of the system (4.8).
From the center manifold theorem, one can say that there exists a center manifold for the system (4.8), which can be locally represented as

$$
\begin{aligned}
\mathbb{W}^c = \Big\{&(\tilde{x}_1, \tilde{x}_2, \tilde{x}_3, \tilde{x}_4) \in \mathfrak{R}^2 \times \mathfrak{R}^2 \ \Big|\ \tilde{x}_3 = F_1(\tilde{x}_1, \tilde{x}_2),\ \text{and } \tilde{x}_4 = F_2(\tilde{x}_1, \tilde{x}_2) \text{ for } |\tilde{x}_1| < \epsilon_1 \text{ and } |\tilde{x}_2| < \epsilon_2,\\
&F_i(0,0) = DF_i(0,0) = 0\Big\},
\end{aligned}
$$

for $i = 1, 2$ and sufficiently small ϵ_1 and ϵ_2. Therefore, the system (4.8) is restricted to the center manifold given below:

$$\begin{cases} \tilde{x}_1' = \tilde{x}_2 + \mathcal{P}_{20}\tilde{x}_1^2 + \mathcal{P}_{11}\tilde{x}_1 x_2 + \mathcal{P}_{02}\tilde{x}_2^2 + O\big(|\tilde{x}_1, \tilde{x}_2|^2\big), \\ \tilde{x}_2' = \mathcal{Q}_{20}\tilde{x}_1^2 + \mathcal{Q}_{11}\tilde{x}_1\tilde{x}_2 + \mathcal{Q}_{02}\tilde{x}_2^2 + O\big(|\tilde{x}_1, \tilde{x}_2|^2\big). \end{cases} \tag{4.9}$$

Using the transformation

$$\begin{cases} \tilde{x}_1' = \mathcal{W} + \frac{1}{2}\big(\mathcal{P}_{11} + \mathcal{Q}_{02}\big)\mathcal{W}^2 + \mathcal{P}_{02}\mathcal{W}\mathcal{V} + O\Big(\big|\mathcal{W}, \mathcal{V}\big|^2\Big), \\ \tilde{x}_2' = \mathcal{V} - \mathcal{P}_{20}\mathcal{W}^2 + \mathcal{Q}_{02}\mathcal{W}\mathcal{V} + O\Big(\big|\mathcal{W}, \mathcal{V}\big|^2\Big), \end{cases}$$

and rewrite the system (4.9), we get

$$\begin{cases} \tilde{x}_1' = \tilde{x}_2, \\ \tilde{x}_2' = \mathcal{Q}_{20}\tilde{x}_1^2 + \mathcal{Q}_{11}\tilde{x}_1\tilde{x}_2 + O\Big(\big|\tilde{x}_1, \tilde{x}_2\big|^2\Big), \end{cases}$$

where $\mathcal{Q}_{20} = \mathcal{Q}_{20}$ and $\mathcal{Q}_{11} = \mathcal{Q}_{11} + 2\mathcal{P}_{20}$. Thus, we have the following theorem:

Theorem 7. *If $\mathcal{Q}_{20} \neq 0$ and $\mathcal{Q}_{11} \neq 0$, then model system* (2.1) *manifests Bogdanov-Takens singularity of co-dimension* 2 *around the endemic equilibrium E_3^*.*

5. Model with delay ($\tau > 0$)

It is well-known that the proposal for the creation of new hospital beds is based on the assessment of current data on infected individuals, but, this process of establishing new hospital beds requires a lot of effort, time, and money. This requirement may lead to some time lag between the construction of new hospital beds and the current data of infected individuals. Thus for the proper arrangement of new hospital beds, it is more reasonable to consider time lag in the increment of newly created hospital beds. In this regard, we have considered that at time t, the increment in new hospital beds is in accordance with the number of infected individuals reported at time $t - \tau$ (for some $\tau > 0$). Taking this into account, the dynamics of model in presence of delay can be expressed by the following system:

$$\begin{cases} \dfrac{dS}{dt} = A - \beta S I - dS + \nu I + \nu_1 H, \\ \dfrac{dI}{dt} = \beta S I - (\nu + \alpha + d)I - k_1(H_a + H_b - H)I, \\ \dfrac{dH}{dt} = k_1(H_a + H_b - H)I - (d + \theta\alpha + \nu_1)H, \\ \dfrac{dH_b}{dt} = \phi I(t - \tau) - \phi_0 H_b. \end{cases} \tag{5.1}$$

Here, $S(0) = S_0 > 0$, $I(\varepsilon) = I_0 \geq 0$ for $\varepsilon \in [-\tau, 0)$, $H(0) = H_0 \geq 0$ and $H_b(0) = H_{b_0} \geq 0$.

5.1. Stability analysis

This section aims to study the stability behavior of endemic equilibrium E_1^* of model system (5.1) in presence of time delay and also explore the possibility of Hopf-bifurcation at the equilibrium E_1^* by taking τ as a bifurcation parameter [40]. For this, we first linearize the model system (5.1) about the endemic equilibrium $E_1^*(S_1^*, I_1^*, H_1^*, H_{b_1}^*)$ by using the following transformations: $S(t) = S_1^* + s(t)$, $I(t) = I_1^* + i(t)$, $H(t) = H_1^* + h(t)$, and $H_b(t) = H_{b_1}^* + h_b(t)$. Thus, the linear system of model system (5.1) around the equilibrium E_1^* is given as follows:

$$\frac{d\vartheta}{dt} = Q_1\vartheta(t) + Q_2\vartheta(t-\tau), \tag{5.2}$$

where $\vartheta = [s(t), i(t), h(t), h_b(t)]^\top$, $Q_1 = \begin{bmatrix} -(\beta I_1^* + d) & -(\beta S_1^* - \nu) & \nu_1 & 0 \\ \beta I_1^* & 0 & k_1 I_1^* & -k_1 I_1^* \\ 0 & k_1(H_a + H_{b_1}^* - H_1^*) & -(d + \theta\alpha + \nu_1 + k_1 I_1^*) & k_1 I_1^* \\ 0 & 0 & 0 & -\phi_0 \end{bmatrix}$, and $Q_2 = \begin{bmatrix} 0 & 0 & 0 & 0 \\ 0 & 0 & 0 & 0 \\ 0 & 0 & 0 & 0 \\ 0 & \phi & 0 & 0 \end{bmatrix}$. Therefore, the linearized system (5.2) has the characteristic equation as follows:

$$\varphi^4 + \varrho_1\varphi^3 + \varrho_2\varphi^2 + \varrho_3\varphi + \varrho_4 + (\varsigma_1\varphi^2 + \varsigma_2\varphi + \varsigma_3)e^{-\varphi\tau} = 0, \tag{5.3}$$

where,

$$\begin{aligned}
\varrho_1 &= 2d + \theta\alpha + \nu_1 + \phi_0 + k_1 I_1^* + \beta I_1^*, \\
\varrho_2 &= (\beta I_1^* + d + \phi_0)(d + \theta\alpha + \nu_1 + k_1 I_1^*) + \phi_0(\beta I_1^* + d) + \beta I_1^*(\beta S_1^* - \nu) - k_1^2 I_1^*(H_a + H_{b_1}^* - H_1^*), \\
\varrho_3 &= \phi_0(\beta I_1^* + d)(d + \theta\alpha + \nu_1 + k_1 I_1^*) + \beta\phi_0 I_1^*(\beta S_1^* - \nu) + \beta I_1^*[(\beta S_1^* - \nu)(d + \theta\alpha + \nu_1 + k_1 I_1^*) - k_1\nu_1(H_a + H_{b_1}^* - H_1^*)] \\
&\quad - k_1^2 I_1^*(H_a + H_{b_1}^* - H_1^*)(\beta I_1^* + d + \phi_0), \\
\varrho_4 &= \beta\phi_0 I_1^*[(\beta S_1^* - \nu)(d + \theta\alpha + \nu_1 + k_1 I_1^*) - k_1\nu_1(H_a + H_{b_1}^* - H_1^*)] - k_1^2\phi_0 I_1^*(\beta I_1^* + d)(H_a + H_{b_1}^* - H_1^*), \\
\varsigma_1 &= k_1\phi I_1^*,\ \varsigma_2 = k_1\phi I_1^*(2d + \theta\alpha + \nu_1 + k_1 I_1^* + \beta I_1^*) - k_1^2\phi I_1^{*2},\ \varsigma_3 = k_1\phi I_1^*(\beta I_1^* + d)(d + \theta\alpha + \nu_1 + k_1 I_1^*) \\
&\quad - k_1\phi I_1^{*2}[k_1(\beta I_1^* + d) + \nu_1\beta].
\end{aligned}$$

Now, to show the occurrence of Hopf-bifurcation, the Eq (5.3) must have a pair of purely imaginary roots. Thus, we substitute, $\varphi = i\eta$ ($\eta > 0$) in Eq (5.3) and separate real and imaginary parts, we have the following equations:

$$\eta^4 - \varrho_2\eta^2 + \varrho_4 = -\varsigma_2\eta\sin\eta\tau - (\varsigma_3 - \varsigma_1\eta^2)\cos(\eta\tau), \tag{5.4}$$

$$\varrho_1\eta^3 - \varrho_3\eta = \varsigma_2\eta\cos(\eta\tau) - (\varsigma_3 - \varsigma_1\eta^2)\sin(\eta\tau). \tag{5.5}$$

Substituting $\eta^2 = \omega$ in the sum of square of Eqs (5.4) and (5.5), we obtain fourth degree polynomial equation in ω as follows:

$$\mathcal{P}(\omega) = \omega^4 + \mathcal{G}_1\omega^3 + \mathcal{G}_2\omega^2 + \mathcal{G}_3\omega + \mathcal{G}_4 = 0, \tag{5.6}$$

here $\mathcal{G}_1 = \varrho_1^2 - 2\varrho_2$, $\mathcal{G}_2 = \varrho_2^2 - 2\varrho_1\varrho_3 + 2\varrho_4 - \varsigma_1^2$, $\mathcal{G}_3 = \varrho_3^2 - 2\varrho_2\varrho_4 - \varsigma_2^2 + 2\varsigma_1\varsigma_3$, $\mathcal{G}_4 = \varrho_4^2 - \varsigma_3^2$.

Now, the nature of solutions of Eq (5.6) is discussed in the following cases:

$\mathcal{P}_1$: If all $\mathcal{G}_i$'s($i = 1, \ldots, 4$) in $\mathcal{P}(\omega)$ are positive then by Descarte's rule of sign, Equation (5.6) posses no real positive root and therefore the Eq (5.3) has no purely imaginary roots for $\tau > 0$. Thus, roots of Eq (5.3) are either negative or contain the negative real part, when $\tau > 0$. Therefore, the following theorem emerges:

Theorem 8. *The equilibrium E_1^*, is locally asymptotically stable for all $\tau > 0$ if E_1^* is feasible, whenever the condition ($\mathcal{P}_1$) is fulfilled, whereas it is stable in presence of delay.*

$\mathcal{P}_2$: If none of the coefficients $\mathcal{G}_i$'s($i = 1, \ldots, 4$) in Eq (5.6) are positive, then by using the Descarte's rule of sign, we can say that the Eq (5.6) has exactly one real positive solution if one of the following conditions holds:

(b_1): $\mathcal{G}_1 > 0, \mathcal{G}_2 > 0, \mathcal{G}_3 > 0$, and $\mathcal{G}_4 < 0$.

(b_2): $\mathcal{G}_1 > 0, \mathcal{G}_2 > 0, \mathcal{G}_3 < 0$, and $\mathcal{G}_4 < 0$.

(b_3): $\mathcal{G}_1 > 0, \mathcal{G}_2 < 0, \mathcal{G}_3 < 0$, and $\mathcal{G}_4 < 0$.

(b_4): $\mathcal{G}_1 < 0, \mathcal{G}_2 < 0, \mathcal{G}_3 < 0$, and $\mathcal{G}_4 < 0$.

If either of the conditions b_i's ($i = 1, \ldots, 4$) is fulfilled, then the Eq (5.3) posses a pair of purely imaginary roots $\pm i\eta_0$. Further, from Eqs (5.4) and (5.5) corresponding to positive value of η_0, we have

$$\tan(\eta_0\tau) = \frac{\Theta_1}{\Theta_2},$$

where, $\Theta_1 = \varsigma_2\eta_0(\eta_0^4 - \varrho_2\eta_0^2 + \varrho_4) + (\varsigma_3 - \varsigma_1\eta_0^2)(\varrho_1\eta_0^3 - \varrho_3\eta_0)$ and $\Theta_2 = (\varsigma_3 - \varsigma_1\eta_0^2)(\eta_0^4 - \varrho_2\eta_0^2 + \varrho_4) - \varsigma_2\eta_0(\varrho_1\eta_0^3 - \varrho_3\eta_0)$. Therefore, the value of τ_m with respect to the positive value of η_0 can be obtained as follows:

$$\tau_m = \frac{m\pi}{\eta_0} + \frac{1}{\eta_0}\tan^{-1}\left(\frac{\Theta_1}{\Theta_2}\right), \text{ for } m = 0, 1, 2, \ldots$$

By taking the advantage of Butler's Lemma [41], one can easily note that the stability of equilibrium E_1^* of model system (2.1) is maintained for $\tau < \tau_0$. Now, to identify, whether the Hopf-bifurcation exists or not as τ increases through τ_0, we prove the following lemma:

Lemma 1. *If condition ($\mathcal{P}_2$) is fulfilled, thus the following condition holds:*

$$sgn\left[\frac{d(\Re(\varphi))}{d\tau}\right]_{\tau=\tau_0} > 0.$$

Proof. Differentiating Eq (5.3), with respect to τ, gives

$$\frac{d\varphi}{d\tau} = \frac{(\varsigma_1\varphi^2 + \varsigma_2\varphi + \varsigma_3)\varphi e^{-\varphi\tau}}{(4\varphi^3 + \varrho_1\varphi^2 + 2\varrho_2\varphi + \varrho_3) + (2\varsigma_1\varphi + \varsigma_2)e^{-\varphi\tau} - (\varsigma_1\varphi^2 + \varsigma_2\varphi + \varsigma_2)\tau e^{-\varphi\tau}}.$$

This gives

$$\left(\frac{d\varphi}{d\tau}\right)^{-1} = \frac{(4\varphi^3 + 3\varrho_1\varphi^2 + 2\varrho_2\varphi + \varrho_3) + (2\varsigma_1\varphi + \varsigma_2)e^{-\varphi\tau}}{\varphi(\varsigma_1\varphi^2 + \varsigma_2\varphi + \varsigma_3)e^{-\varphi\tau}} - \frac{\tau}{\varphi}.$$

This implies that

$$\begin{aligned} sgn\left[\frac{d(\Re(\varphi))}{d\tau}\right]_{\tau=\tau_0} &= sgn\left[\frac{d(\Re(\varphi))}{d\tau}\right]^{-1}_{\tau=\tau_0} \\ &= sgn\left[\Re\frac{d(\varphi)}{d\tau}\right]_{\varphi=i\eta_0} \\ &= sgn\left[\frac{4\eta_0^6 + 3\mathcal{G}_1\eta_0^4 + 2\mathcal{G}_2\eta_0^2 + \mathcal{G}_3}{\varsigma_2^2\eta_0^2 + (\varsigma_3 - \varsigma_1\eta_0^2)^2}\right] \\ &= sgn\left[\frac{\mathcal{P}'(\eta_0^2)}{\varsigma_2^2\eta_0^2 + (\varsigma_3 - \varsigma_1\eta_0^2)^2}\right] \end{aligned}$$

Thus, it can be noted that $\mathcal{P}'(\eta_0^2) > 0$ if one of the conditions (b_i)'s $(i = 1, \ldots, 4)$ is satisfied. This proves the Lemma 1.

Thus, the following result emerges:

Theorem 9. *If conditions* (3.3) *holds and any one of the conditions* (b_i)*'s* $(i = 1, \ldots, 4)$ *is fulfilled, then equilibrium* E_1^* *is locally asymptotically stable for all* $\tau \in [0, \tau_0)$ *and trn into unstable for* $\tau > \tau_0$*. The model system* (5.1) *manifests a supercritical Hopf-bifurcation when* $\tau = \tau_0$*, generating a family of periodic solutions bifurcating from equilibrium* E_1^* *as* τ *crosses* τ_0 *[42].*

Remark 1. *Further, if none of the conditions* (b_i)*'s* $(i = 1, \ldots, 4)$ *is satisfied, then it is possible that Eq* (5.6) *posses more than one positive roots. In this case, Equation* (5.3) *exhibits pair of two purely imaginary roots. Therefore, we numerically deliberate the result for which Eq* (5.6) *posses two real positive roots.*

$\mathcal{P}_3$: Analytically, the condition for which Eq (5.6) posses two real positive real roots is not easy to obtain, i.e., Equation (5.3) has two pair of purely imaginary roots. So, we discuss the result numerically in which Eq (5.6) has two positive real roots. Numerically, it is obtained that the Eq (5.6) has two positive real roots ω_+ (corresponding to η_+^2) and ω_- (corresponding to η_-^2) where $\omega_+ > \omega_-$, i.e., the characteristic Eq (5.3) has two pairs of purely imaginary roots $\pm i\eta_\pm$. For these positive values of $\eta_\pm$, from Eqs (5.4) and (5.5) we can obtain the positive value of $\tau_m^\pm$ as follows:

$$\tau_m^\pm = \frac{1}{\eta_\pm}\tan^{-1}\left[\frac{\varsigma_2\eta_\pm(\eta_\pm^4 - \varrho_2\eta_\pm^2 + \varrho_4) + (\varsigma_3 - \varsigma_1\eta_\pm^2)(\varrho_1\eta_\pm^3 - \varrho_3\eta_\pm)}{(\varsigma_3 - \varsigma_1\eta_\pm^2)(\eta_\pm^4 - \varrho_2\eta_\pm^2 + \varrho_4) - \varrho_2\eta_\pm(\varrho_1\eta_\pm^3 - \varrho_3\eta_\pm)}\right] + \frac{(2m+1)\pi}{\eta_\pm} \text{ for } m = 0, 1, 2, 3, \ldots$$

Using the Butler's lemma [41], one can easily note that the equilibrium E_1^* of model system (5.1) remains stable for $\tau < \tau_m^+$ and unstable for $\tau < \tau_m^-$.

Now, to analyze whether the Hopf-bifurcation arises or not as τ passes through $\tau_m^{\pm}$, we have to prove the following lemma:

Lemma 2. *If Eq* (5.6) *contains two real positive real solutions, then the following conditions are hold:*

$$sgn\left[\frac{d(\Re(\varphi))}{d\tau}\right]_{\tau=\tau_m^+} > 0, \text{ and } sgn\left[\frac{d(\Re(\varphi))}{d\tau}\right]_{\tau=\tau_m^-} < 0,$$

Proof. Differentiating (5.3), with respect to τ, we obtained

$$\begin{aligned} sgn\left[\frac{d(\Re(\varphi))}{d\tau}\right]_{\tau=\tau_m^{\pm}} &= sgn\left[\frac{d(\Re(\varphi))}{d\tau}\right]^{-1}_{\tau=\tau_m^{\pm}} \\ &= sgn\left[\Re\frac{d(\varphi)}{d\tau}\right]_{\varphi=i\eta_{\pm}} \\ &= sgn\left[\frac{4\eta_{\pm}^6 + 3\mathcal{G}_1\eta_{\pm}^4 + 2\mathcal{G}_2\eta_{\pm}^2 + \mathcal{G}_3}{\varsigma_2^2\eta_{\pm}^2 + (\varsigma_3 - \varsigma_1\eta_{\pm}^2)^2}\right] \\ &= sgn\left[\frac{\mathcal{P}'(\eta_{\pm}^2)}{\varsigma_2^2\eta_{\pm}^2 + (\varsigma_3 - \varsigma_1\eta_{\pm}^2)^2}\right]. \end{aligned}$$

Hence, if Eq (5.6) contains two real positive roots then $\mathcal{P}'(\omega_+^2) > 0$ and $\mathcal{P}'(\omega_-^2) < 0$ and therefore the transversality conditions hold. This concludes the proof of Lemma 2.

Thus, the following result emerges regarding the Hopf-bifurcation theorem of functional differential equation [42], which is stated as follows:

Theorem 10. *If Eq* (5.6) *contains two real positive solutions and condition* (3.3) *is fulfilled, then a positive integer $\tilde{q}$ exists, for which $\tilde{q}$ stability switches occur from stability to instability and later the system becomes unstable. More specifically, when $\tau \in [0, \tau_0^+), (\tau_0^-, \tau_1^+), \ldots, (\tau_{\tilde{q}-1}^-, \tau_{\tilde{q}}^+)$, the equilibrium E_1^* is stable while it is unstable when $\tau \in (\tau_0^+, \tau_0^-), (\tau_1^+, \tau_1^-), \ldots, (\tau_{\tilde{q}-1}^+, \tau_{\tilde{q}-1}^-)$.*

6. Numerical simulations

The qualitative behavior of the system (2.1) around equilibrium has been discussed in previous sections to comprehend the disease dynamics and get insights into the feasibility of equilibria, their local stability, and Hopf-bifurcation in absence as well as in the presence of delay. We have also identified the existence of transcritical, saddle-node, and BT-bifurcation in the absence of delay. To simulate the model system (2.1), we choose a set of hypothetical parameter values given in Table 1.

For the hypothetically chosen set of parameter values in Table 1, the existence conditions for equilibrium E_1^* are fulfilled and basic reproduction number is $R_0 = 5.614 > 1$. Also, the components of endemic equilibrium E_1^* is obtained as

$$S_1^* \approx 125 \text{ persons}, \; I_1^* \approx 77 \text{ persons}, \; H_1^* \approx 247 \text{ persons}, \; H_{b_1}^* \approx 154 \text{ new hospital beds}$$

First, to see the effect of newly created hospital beds on infected individuals' death due to infection, we generate a bar graph with $k_1 = 0.00002$ and varying the increment rate of new hospital beds (ϕ)

from 0.01 to 0.046 (Figure 1). This figure shows the change in percentage of susceptible (blue bar), infected (green), hospitalized (yellow), and deaths due to infection for different values of ϕ. One can easily observe that as we increase the increment rate of new hospital beds, will increase the percentage of the hospitalized population as well as decrease the percentage of infected individuals and deaths due to infection.

Table 1. Parameter description of model system (2.1) and their considered values used for numerical simulation.

Parameter	Description	Value
A	Immigration rate	20 day^{-1}
β	Transmission rate of individuals from susceptible class to infected class	2×10^{-3} person^{-1}day^{-1}
k_1	Hospital bed occupancy rate	5×10^{-3} day^{-1}
d	Natural mortality rate	0.01 day^{-1}
ν	Self recovery rate	2.5×10^{-3} day^{-1}
ν_1	Hospital recovery rate	2×10^{-3} day^{-1}
H_a	Total number of hospital beds	100
α	Disease induced mortality rate	0.2 day^{-1}
ϕ	increment rate of new hospital beds	0.02 day^{-1}
ϕ_0	the rate at which hospital beds reduces	0.01 day^{-1}
θ	Disease induced mortality coefficient of hospitalized individuals	0.1×10^{-3}

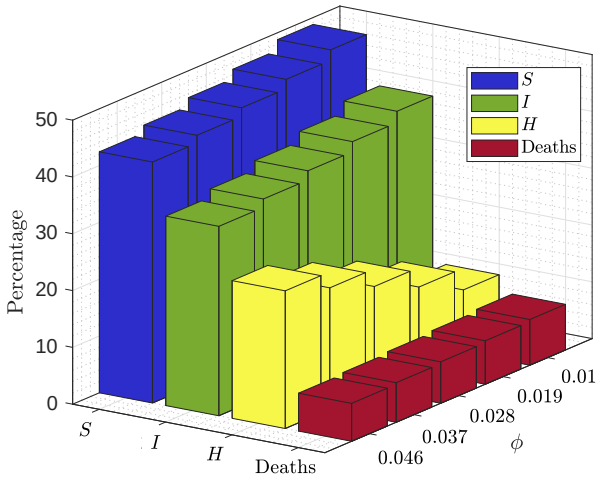

Figure 1. The graphical representation of the change in percentage of disease-induced deaths (blue), hospitalized (yellow), infected (green), and susceptible (green) individuals for different increment rates of newly created hospital beds with $k_1 = 0.00002$.

Further, we plot equilibrium curve in $R_0 - I$ plane to demonstrate the different dynamics of model system (2.1). First, when we choose $k_1 = 0.0007$, the model system (2.1) displays the transcritical bifurcation in forward direction, Figure 2(a). This figure reveals that when basic reproduction number $R_0 > 1$, the disease will persist in the population and eventually go extinct when $R_0 < 1$. Further, when we increase the hospital occupancy rate to $k_1 = 0.0011$, the direction of transcritical bifurcation

changes in backward, which fledges a complex situation, Figure 2(b). From this figure, we can see that two equilibrium points (one stable and one unstable) will collide and unite into one equilibrium point when the equilibrium curve reaches its turning point and disappear thereafter, which shows that the model system (2.1) exhibits saddle-node bifurcation at that turning point (marked with SN in Figure 2(b)). It can also be seen from this figure that the system exhibits a bistable case when $R_0 \in (R_c, 1)$, which means the disease will persist or not in the population is entirely dependent on the initial population of infected individuals. Also, keeping R_0 less than the R_c will be necessary to eradicate the disease from the population.

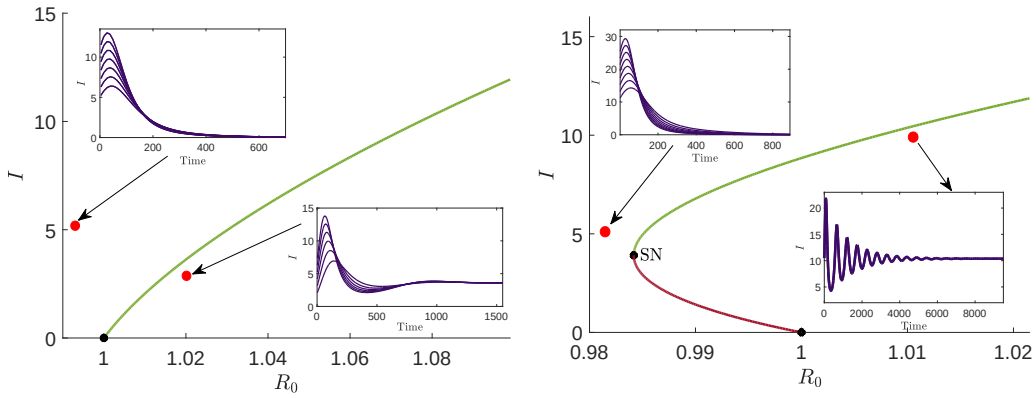

Figure 2. Bifurcation plot in $R_0 - I$ plane for model system (2.1). (a) forward bifurcation occurs when $k_1 = 0.0007$, (b) backward bifurcation occurs for $k_1 = 0.0011$. The green curve indicates equilibrium points that are stable, and the brown curve indicates equilibrium points that are unstable. The violet curves represent the time series plot of infected individuals generated for the value of basic reproduction number indicated with red dots.

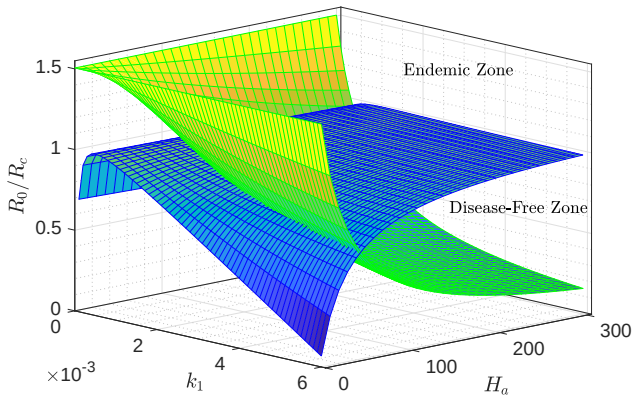

Figure 3. Surface plot of basic reproduction number (R_0) and its threshold (R_c) with $\beta = 0.00016$. The green surface represents basic reproduction number and blue surface represents its critical value R_c.

Furthermore, for the chosen set of parameter values except $\beta = 0.0016$, we generate the surface plot of basic reproduction number R_0 and its threshold quantity R_c by varying the hospital occupancy rate k_1 (0–6×10^{-3}) and total number of hospital beds H_a (0–300), Figure 3. From this figure, we can observe that with the increment in hospital occupancy rate, an increment in the number of hospital beds becomes necessary to eradicate the disease.

When we generate the equilibrium curve in $R_0 - I$ plane with hospital occupancy rate $k_1 = 0.001212$, model system (2.1) exhibits two Hopf-points H_1 (at $R_0 \approx 0.9771$) and H_2 (at $R_0 \approx 0.9956$), Figure 4(a). From this figure, we observe that if $R_0 < 0.97134$ (SN point), the disease will die out from the population, on the other hand, if $R_0 \in (0.97137, 0.977083)$ or $R_0 \in (0.995607, 1)$ the disease will persist or extinct from the population will depend on the initial size of the infected individuals. Further, between Hopf-points H_1 and H_2 model system (2.1) enters into limitcycle oscillation by forward supercritical Hopf-bifurcation and disappears via backward supercritical Hopf-bifurcation. This dramatic behavioral change of the model system will make the situation unpredictable between H_1 and H_2; thus, to make any decision to control the prevalence of disease, we have to reduce R_0 below 0.97710 or increase above 1. Furthermore, when we increase the value of hospital occupancy rate to 0.00125, the model system (2.1), exhibits supercritical Hopf-bifurcation at $R_0 = 1.01585$ and disappear via Homoclinic bifurcation, Figure 4(b).

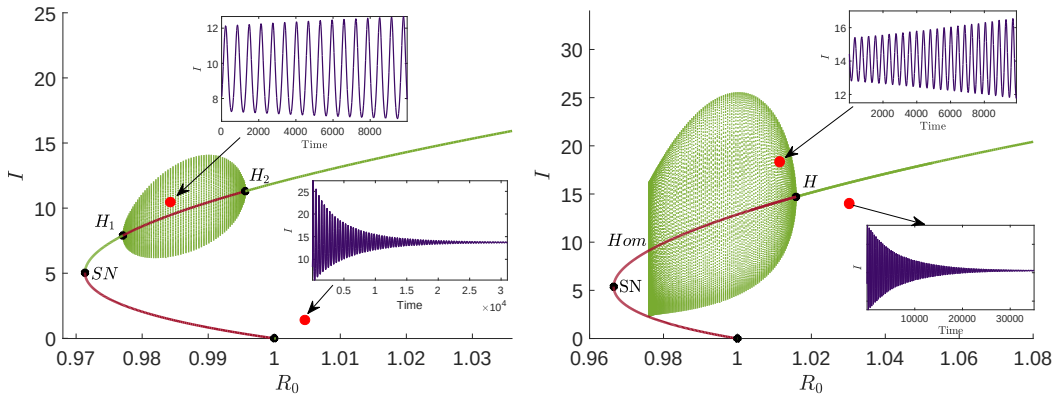

(a) (b)

Figure 4. Bifurcation plot in $R_0 - I$ plane for model system (2.1). (a) $k_1 = 0.001212$, (b) $k_1 = 0.00125$. The green curve indicates equilibrium points that are stable, and the brown curve indicates equilibrium points that are unstable. The violet curves represent the time series plot of infected individuals, generated for the value of basic reproduction number indicated with red dots.

Further, for $k_1 = 0.0028$, the model system exhibits limitcycle bifurcation, Figure 5(a). This figure evinces that when $R_0 < 1.0402$ the endemic equilibrium E_1^* violates the condition of stability and surrounds itself with a stable limitcycle. Also, for $R_0 > 1.0402$, the stable endemic equilibrium E_1^* surrounds itself with two limit cycles, from which one is stable, and another is unstable, and these two limit cycles collide, unite and disappear via limitcycle bifurcation when $R_0 \approx 1.1388$. To get the clear idea about limitcycle bifurcation, we generate the bifurcation plot in $R_0 - S - I$ space, Figure 5(b).

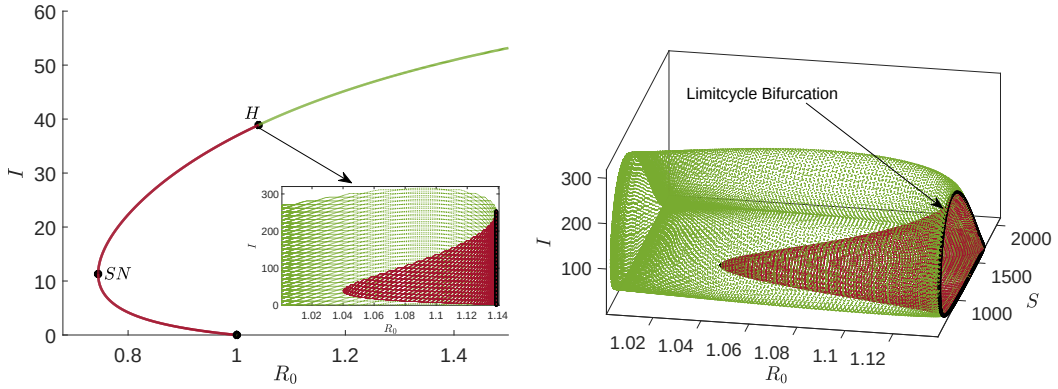

Figure 5. Bifurcation plot for model system (2.1) when $k_1 = 0.0028$ in (a) $R_0 - I$ plane and (b) $R_0 - S - I$ space. The green curve indicates equilibrium points (limitcycles) that are stable, and the brown curve indicates equilibrium points (limitcycles) that are unstable.

For $k_1 = 0.0085$ model system (2.1) showcase the subcritical bifurcation and disappear through homoclinic bifurcation, Figure 6(a). This figure reveals that for $R_0 > 0.6271$ the stable endemic equilibrium E_1^* surrounds with the unstable limitcycles, but for $R_0 < 0.6271$, endemic equilibria E_1^* and E_2^* both become unstable. The bifurcation plot in $R_0 - S - I$ space is shown in Figure 6(b).

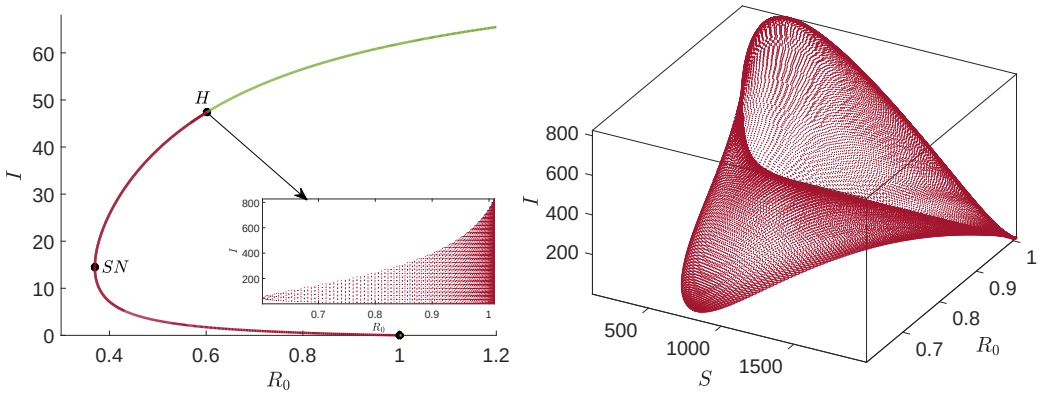

Figure 6. Bifurcation plot for model system (2.1) when $k_1 = 0.0085$ in (a) $R_0 - I$ plane and (b) $R_0 - S - I$ space. The green curve indicates equilibrium points (limitcycles) that are stable, and the brown curve indicates equilibrium points (limitcycles) that are unstable.

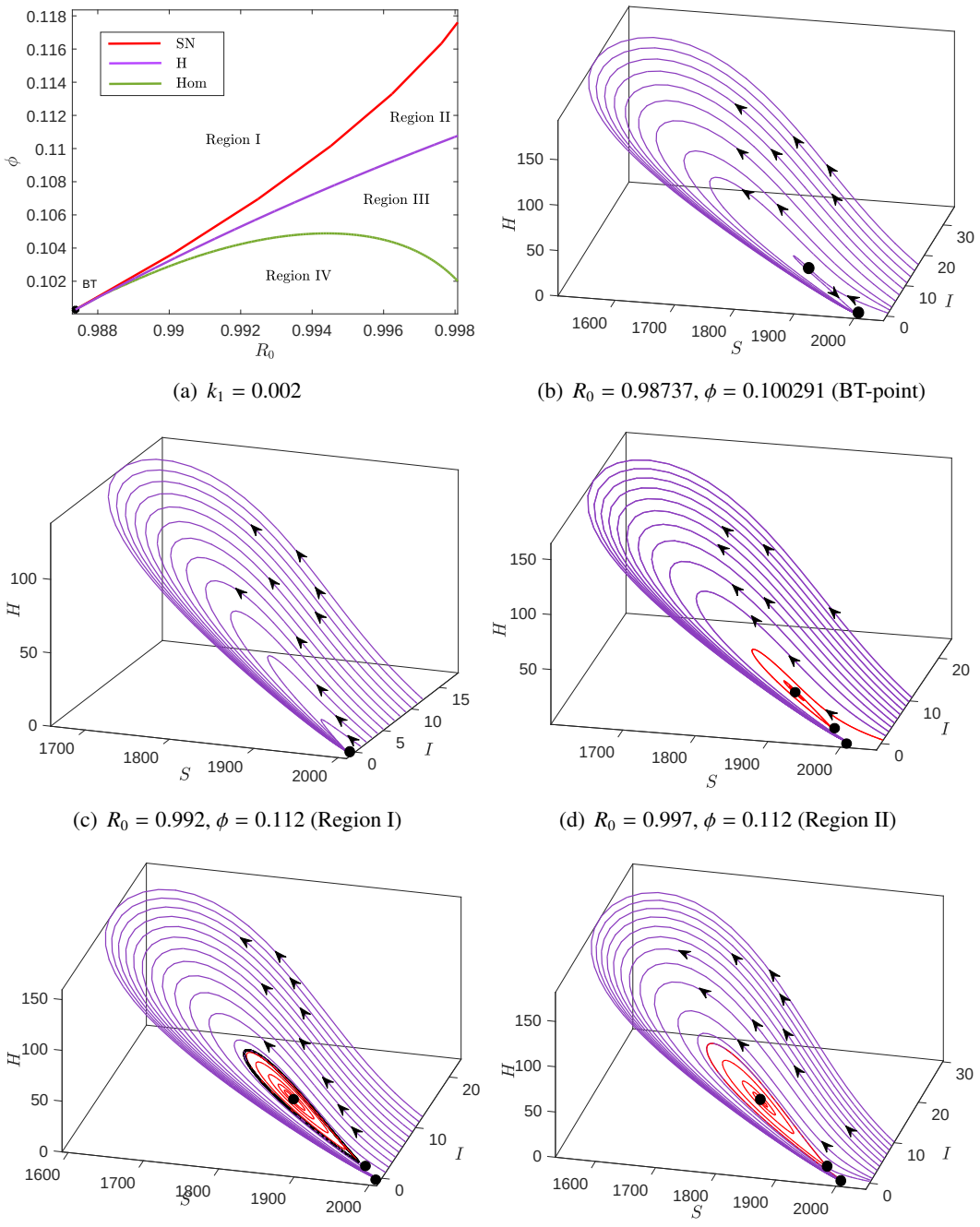

(a) $k_1 = 0.002$

(b) $R_0 = 0.98737$, $\phi = 0.100291$ (BT-point)

(c) $R_0 = 0.992$, $\phi = 0.112$ (Region I)

(d) $R_0 = 0.997$, $\phi = 0.112$ (Region II)

(e) $R_0 = 0.997$, $\phi = 0.106$ (Region III)

(f) $R_0 = 0.996$, $\phi = 0.102$ (Region IV)

Figure 7. (a) Bifurcation plot in $R_0 - \phi$ Plane, (b)–(f) Phase Portrait in $S - I - H$ space.

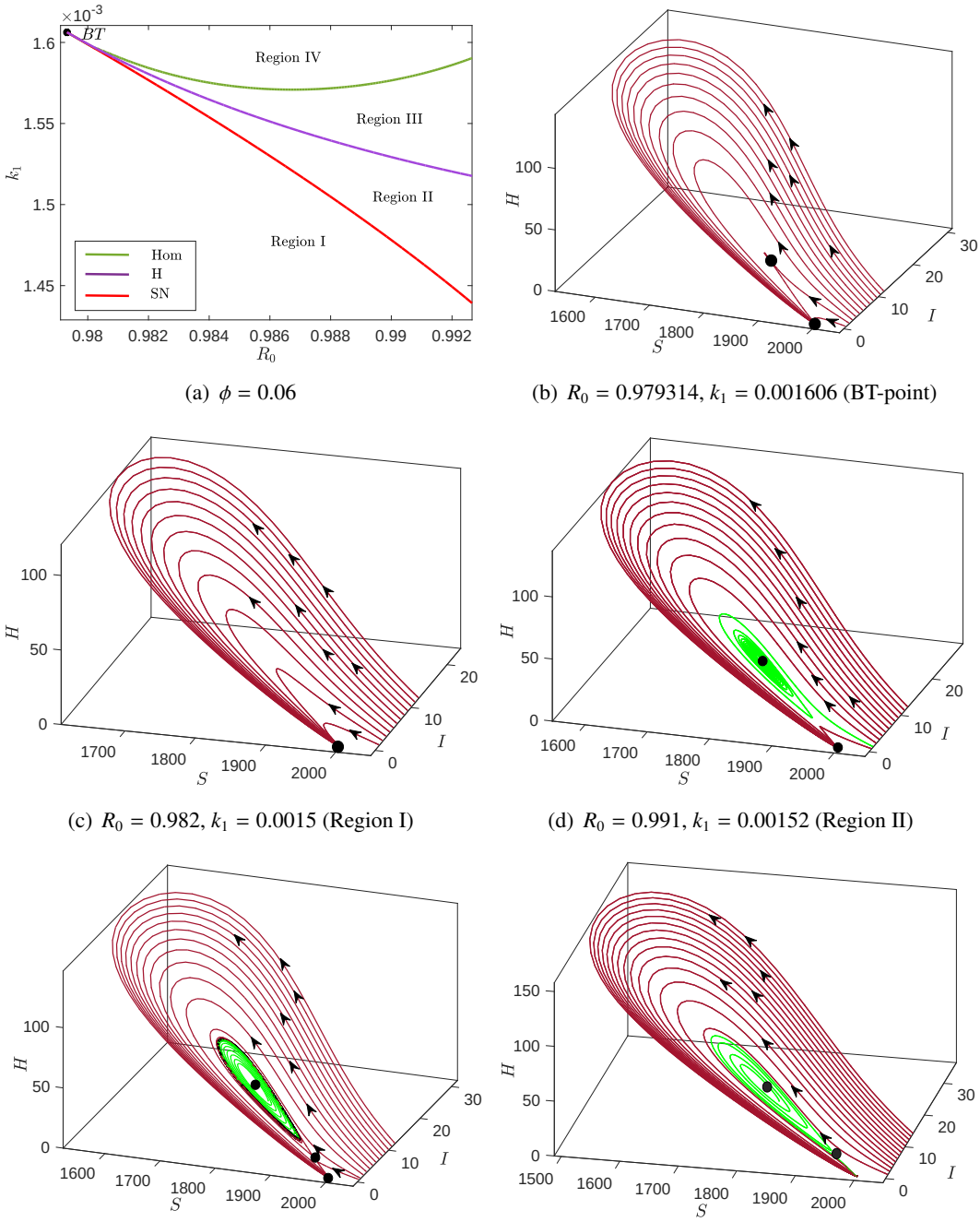

(a) $\phi = 0.06$

(b) $R_0 = 0.979314$, $k_1 = 0.001606$ (BT-point)

(c) $R_0 = 0.982$, $k_1 = 0.0015$ (Region I)

(d) $R_0 = 0.991$, $k_1 = 0.00152$ (Region II)

(e) $R_0 = 0.991$, $k_1 = 0.00155$ (Region III)

(f) $R_0 = 0.988$, $k_1 = 0.00159$ (Region IV)

Figure 8. (a) Bifurcation plot in $R_0 - k_1$ Plane, (b)–(f) Phase Portrait in $S - I - H$ space.

To show the existence of BT-bifurcation of co-dimension 2, we have plot the bifurcation diagram in $R_0 - \phi$, Figure 7(a). This algebraic curve in $R_0 - \phi$ represents the bifurcation plot near the BT-point (0.987376, 0.100291) at which the components of endemic equilibrium are (1920.168, 2.2247, 33.0449, 22.3125). From Figure 7(a) construct with three curves i.e., saddle-node (SN), Hopf (H) and Homoclinic (Hom) that are represented with red, violet and green color, respectively. These three curve divide the $R_0 - \phi$ plane into four regions (Regions I–IV). The dynamics

of model system (2.1) is different in these four regions. The model system (2.1) exhibits a unique endemic equilibrium at the BT point $(R_0, \phi) = (0.987376, 0.100291)$, which is saddle in nature and a disease-free equilibrium, Figure 7(b). Further, there exists only disease-free equilibrium, when we choose the value of R_0 and ϕ from Region I, i.e., $(R_0, \phi) \approx (0.992, 0.112)$, Figure 7(c). The model system (2.1) exhibits a disease-free equilibrium and two endemic equilibria from which one is stable focus, and another is saddle-node when we consider $(R_0, \phi) \approx (0.997, 0.112)$ (Region II), Figure 7(d). Again two endemic equilibria occurs when we choose the values of R_0 and ϕ from Region III, i.e., $(R_0, \phi) \approx (0.997, 0.106)$, Figure 7(e). From which, one endemic equilibrium is saddle in nature and another is unstable, which surrounds itself with and stable limit cycle. Furthermore, two endemic equilibria, for the values taken from Region IV, i.e., $(R_0, \phi) \approx (0.996, 0.102)$. The endemic equilibrium with high endemicity is unstable and another is saddle-node, Figure 7(f).

Also, to demonstrate the effect of hospital occupancy rate on the disease dynamics, we have plot the bifurcation diagram in $R_0 - k_1$ plane. This algebraic plane again consists of three curve saddle-node, Hopf and homoclinic, which unfold the BT-point, Figure 8(a). The saddle-node (SN), Hopf (H) and Homoclinic (Hom) curves divide the algebraic plane $R_0 - k_1$ in four regions (Regions I–IV). The dynamics of model system (2.1) is different in these four regions.

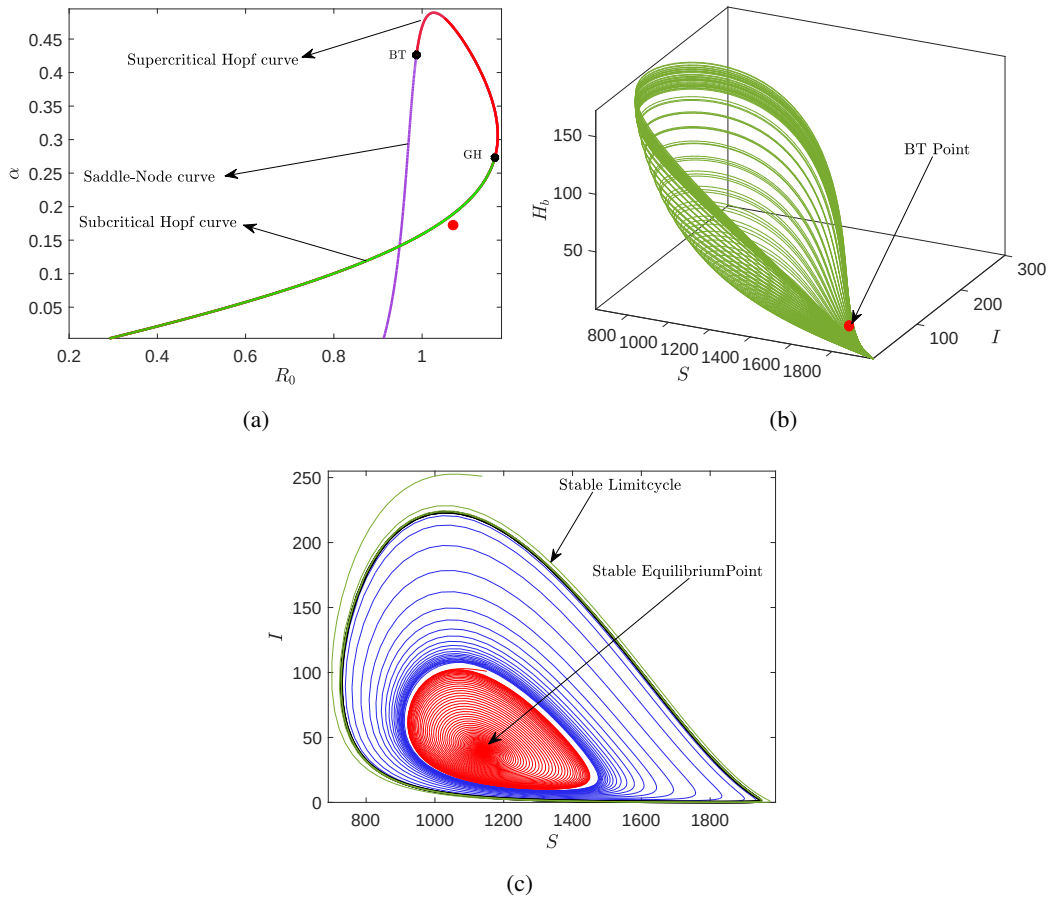

Figure 9. (a) Bifurcation plot in $R_0 - \alpha$ plane for model system (2.1), (b) BT-curve in $S - I - H_b$ space, (c) Phase portrait in $S - I$ plane for the value indicate with red dot in (a).

The model system (2.1), possess a unique endemic equilibrium at the BT point (R_0, k_1) = (0.979314, 0.0.00161), which is saddle in nature and a disease-free equilibrium, Figure 8(b). For $(R_0, k_1) \approx (0.982, 0.0015)$ (Region I), the model system (2.1) exhibits only disease-free equilibrium, Figure 8(c). For $(R_0, k_1) \approx (0.991, 0.00152)$ (Region II), the proposed system (2.1) has two endemic equilibria from which one is stable focus, and another is saddle-node, Figure 8(d). When we consider the value of R_0 and k_1 from Region III, i.e., $(R_0, k_1) \approx (0.991, 0.00155)$, Figure 8(e) the model system (2.1) exhibits two endemic equilibria, one is saddle in nature and another is unstable, which surrounds itself with a stable limit cycle. Further, the system has one unstable equilibrium and one saddle-node when we choose the value of R_0 and k_1 from Region IV, i.e., $(R_0, k_1) \approx (0.988, 0.00159)$, Figure 8(f).

Furthermore, when we choose $k_1 = 0.002$ and generate the bifurcation plot in $R_0 - \alpha$ plane, the model system (2.1), showcase the generalized Hopf-bifurcation, Figure 9(a). This figure consists of two points (BT and GH) and three curves (violet, red and green). The points BT and GH sequentially represent the Bogdanov-Takens and generalized Hopf-bifurcation points. At the curve above GH point (green curve), model system (2.1) exhibits supercritical Hopf-bifurcation, and below GH point, sub-critical bifurcation occurs. At the violet curve, the model system undergoes saddle-node bifurcation. The homoclinic curve generated from the BT point in $S - I - H_b$ space is shown in Figure 9(b). The Figure 9(c) shows the phase portrait diagram of model system (2.1) for $R_0 = 1.05$ and $\alpha = 0.168$. This value of R_0 and α is chosen from Figure 9(a) (marked with red dot). From Figure 9(c), one can see that the model system exhibits one stable equilibrium, which surrounds itself with one stable (black curve) and one unstable (between red and blue curve) limitcycles.

6.1. Time-delay model

If we choose $\beta = 0.0003$, $k_1 = 0.0007$, $\phi = 0.08$ and $\phi_0 = 0.04$ and keep remaining parameter values same as in Table 1, the Eq (5.6) possess a unique positive real root, which ensure the existence of pair of purely imaginary roots for Eq (5.2). For the selected data τ_0 is obtained 7.55 days. The bifurcation plot in $\tau - S - I$ space is show in Figure 10. The phase portraits in $S - I - H$ space for $\tau = 5$ days ($< \tau_0 = 7.55$ days) and $\tau = 12$ days ($> \tau_0 = 7.55$ days) are sequentially shown in Figure 11(a),(b). This figure shows that the solution trajectories approaches to the equilibrium value when $\tau < \tau_0$ and stable limitcycle obtained around unstable equilibrium, when $\tau > \tau_0$.

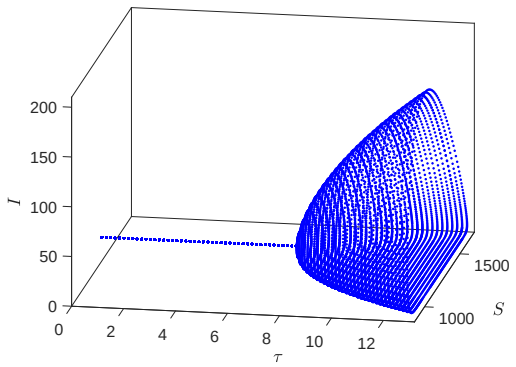

Figure 10. Bifurcation plot in $\tau - S - I$ space.

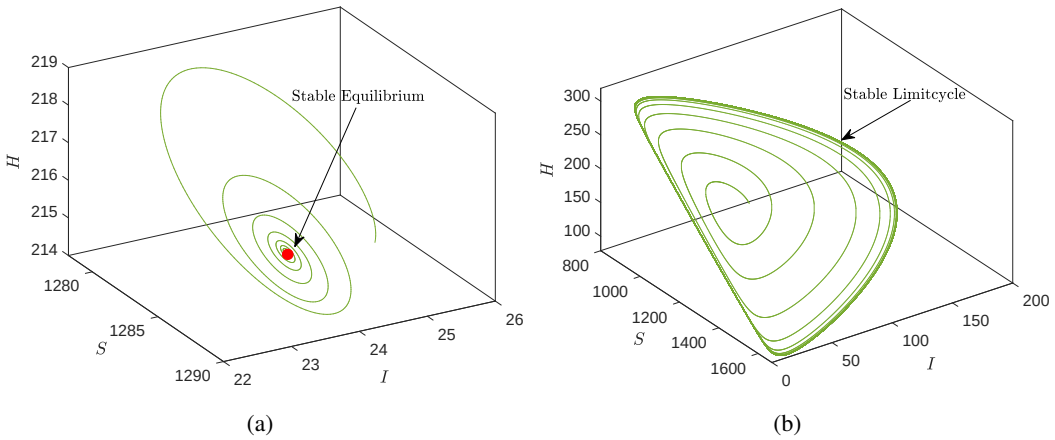

Figure 11. Phase portrait in $S - I - H$ space for (a)$\tau = 5$, (b) $\tau = 12$.

Further, to show the different dynamical changes in the proposed model with time delay in increment of new hospital beds, we have choose $\beta = 0.0005$, $\nu = 0.1$, $\nu_1 = 0.5$, $\alpha = 0.09$, $\phi = 0.08$, $\phi_0 = 0.05$ and the remaining parameter values are same as in Table 1. For these values of parameters, equation (5.6) has exactly two real positive roots i.e., $\omega_+ \approx 0.00722$ and $\omega_- \approx 0.00227$ ($\omega_+ > \omega_-$). Corresponding to these positive roots, the positive values of $\tau_m^{\pm}$ for $k = 1, 2, 3 \ldots$ is obtained. Thus, we have obtained $\tau_0^+ = 19.445$ days, $\tau_1^+ = 93.399$ days, $\tau_2^+ = 167.354$ days, $\tau_3^+ = 241.308$ days and so on and the values of $\tau_0^- = 63.731$, $\tau_1^- = 195.497$, $\tau_2^- = 327.264$, $\tau_3^- = 459.0304$ and so on. Therefore, using Theorem 10, one can observe that for the selected set of data the endemic equilibrium is stable if $\tau \in [0, 19.445) \bigcup (63.7306, 93.399)$ and unstable for $(19.455, 63.7306) \bigcup (93.399, \infty)$. This dynamical change can be seen in bifurcation plot in Figure 12. The phase portraits in $S - I - H$ space for $\tau = 12$, $\tau = 40$, $\tau = 80$ and $\tau = 120$ are sequentially displayed in Figure 13(a)–(d).

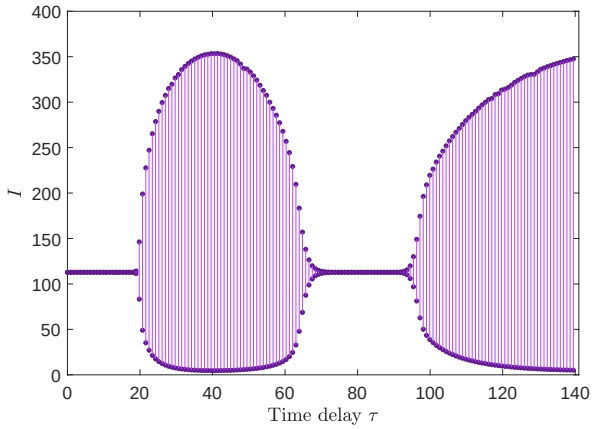

Figure 12. Bifurcation plot in $\tau - I$ plane.

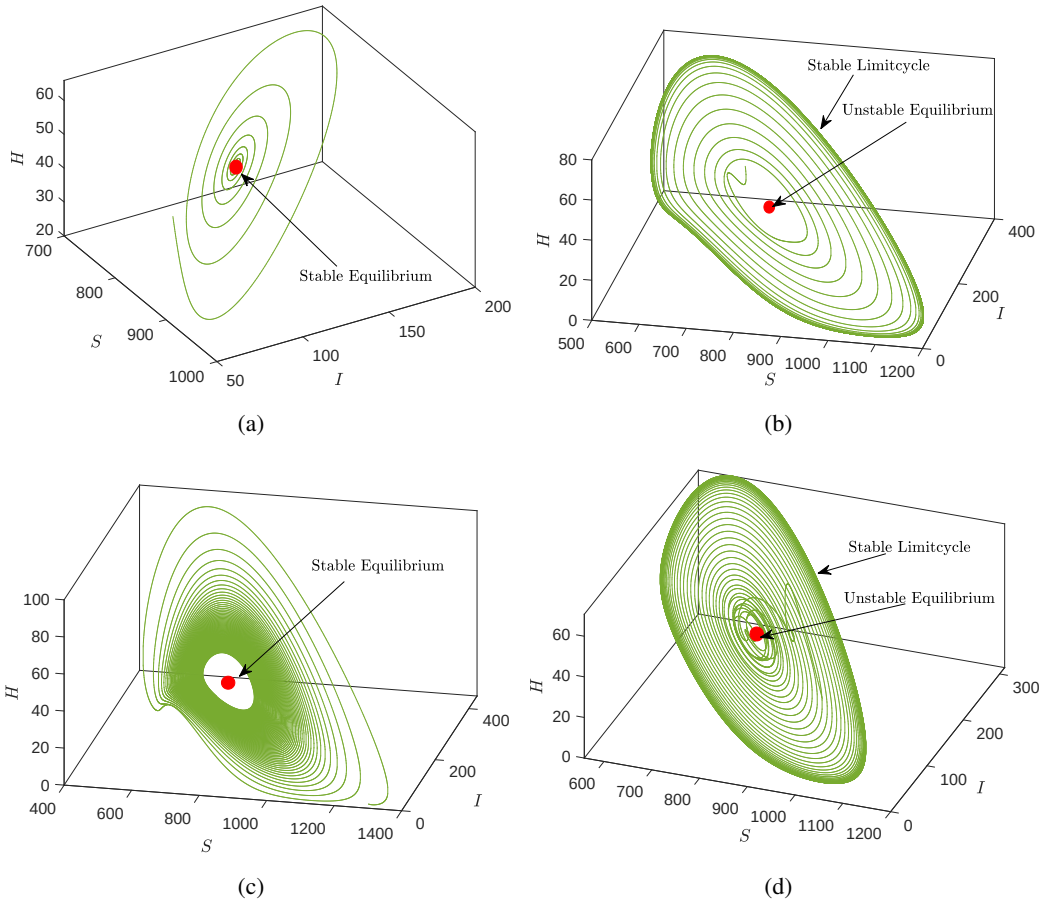

Figure 13. Phase portrait in $S - I - H$ space for (a) $\tau = 12$, (b) $\tau = 40$, (c) $\tau = 80$, (d) $\tau = 120$.

7. Conclusions and future work

To reduce the prevalence of infectious diseases, it is imperative to arrange an adequate number of hospital beds. Still, it is not entirely clear how many hospital beds will be able to achieve the complete eradication of such diseases. Thus, the best way to arrange sufficient hospital beds is to increase the number of hospital beds with the increase in infected individuals. Keeping this goal in mind, this work deals with the four-dimensional nonlinear mathematical model in which the human population is divided into three classes, i.e., susceptible, infected, and hospitalized. The proposed model incorporates the assumption that susceptible individuals become infected via direct contact with infected individuals. Accordingly, it is assumed that the number of hospital beds will increase with an increasing number of individuals infected with the disease. Further, we also consider that the funds involved in the creation of new hospital beds limit the growth rate of newly created beds at a rate ϕ_0.

We begin with a qualitative analysis of the deterministic model. To thoroughly analyze the dynamics of the proposed model with a slight change in considered parameters, we study its bifurcation behavior (i.e., transcritical, saddle-node, Hopf, and BT-bifurcation). From Section 4.1, it is found that whenever $\left(\frac{d+\theta\alpha+\nu_1}{k_1(k_1d+\beta^*\nu_1)}\right)\left[\beta^*\left(\frac{\beta^*A}{d}-\nu\right)+k_1d\frac{\phi}{\phi_0}\right] < H_a$, the system manifests transcritical bifurcation in

the backward direction, which means the classical requirement to eliminate the disease from the population will contravene, and disease may persist even if $R_0 < 1$. Also, the proposed (2.1) demonstrates saddle-node bifurcation, whenever $k_1 \neq \frac{\beta_c(d+\theta\alpha)}{d}$, and $H^*_{b_3} \neq H^*_3$. For the local representation of homoclinic bifurcation, we deduced the normal form around the endemic equilibrium E^*_3. We have also obtained the periodic pattern for the model system (2.1). The model system (2.1) becomes unstable around the endemic equilibrium for high hospital occupancy rates (k_1), resulting in multiple Hopf-bifurcations, the first being supercritical and the second is subcritical. Through subcritical Hopf-bifurcation, we have also dissected the possibility of multiple limitcycles and limitcycle bifurcation, Figure 5.

It is clear from the results obtained in this study that the increase in hospital beds becomes very important as the number of infected individuals increases. From Figure 1, it can be easily noted that the percentage of infected individuals and deaths due to the infection can be significantly reduced to 1.372 and 6.86 percent, respectively, when the increment rate of new hospital beds increased from 0.01 to 0.046. Thus, the increment of new hospital beds can reduce deaths caused by they infection.

In order to predict more realistic dynamics for the proposed system, we have also added a time delay in the increase of new beds. We have also discussed the stability behavior of equilibrium E^*_1 and existence of Hopf bifurcation around it, in the presence of time delay. It is observed that the introduction of time delay changes the dynamics of the system as delay parameter crosses a critical threshold for one set of parameter values of τ (i.e., $\tau \in [0, \tau_0)$). The periodic oscillations with increasing amplitude have been observed when we increase the value of the time delay above the threshold (τ_0), i.e., the endemic equilibrium E^*_1 becomes unstable. The system switches between stability and instability for another set of parameter values and eventually, it turns into unstable. The study reveals that to control an epidemic outbreak, the sufficient number of hospital beds are necessary. The delay in adding new beds to hospitals may destabilize the system and lead to stability switches via Hopf-bifurcation, which makes it difficult to predict and control the prevalence of infection. Hence, the addition of new hospital beds on time is necessary to control the transmission of infectious disease.

In the present paper, we have focused on the hospital bed's incrementation and its impact on emerged disease dynamics. For our model, we have assumed that the hospital beds are increased proportional to the number of infected individuals. However, limited resource availability may affect this increment. Thus, a separate differential equation could be included in the model to describe this limitation of resource availability. Meanwhile, it is essential to link the cost associated with the new hospital beds. These topics may be considered in future. The impact of other pharmaceutical interventions like vaccine, medicines, transport facilities of hospitals, etc. can also be studied in future.

Acknowledgments

The researchers would like to thank the Deanship of Scientific Research, Qassim University for funding the publication of this project.

Conflict of interest

There are no conflicts of interest disclosed by the authors.

References

1. *Hospital Bed Population Ratio (HBPR), OECD Data*, Available from: https://data.oecd.org/healtheqt/hospital-beds.htm.
2. *Hospital Bed Population Ratio (HBPR) in Saudi Arabia, The World Bank Data*, Available from: https://data.worldbank.org/indicator/SH.MED.BEDS.ZS?locations=SA.
3. *World Health Organization*, *World Health Statistics*, 2005–2015.
4. P. Das, R. K. Upadhyay, A. K. Misra, F. A. Rihan, P. Das, D. Ghosh, Mathematical model of COVID-19 with comorbidity and controlling using non-pharmaceutical interventions and vaccination, *Nonlinear Dyn.*, **106** (2021), 1213–1227. https://doi.org/10.1007/s11071-021-06517-w
5. A. K. Misra, R. K. Rai, P. K. Tiwari, M. Martcheva, Delay in budget allocation for vaccination and awareness induces chaos in an infectious disease model, *J. Biol. Dyn.*, **15** (2021), 395–429. https://doi.org/10.1080/17513758.2021.1952322
6. J. A. T. Machado, J. Ma, Nonlinear dynamics of COVID-19 pandemic: modeling, control, and future perspectives, *Nonlinear Dyn.*, **101** (2020), 1525–1526. https://doi.org/10.1007/s11071-020-05919-6
7. R. Naresh, S. Pandey, A. K. Misra, Analysis of a vaccination model for carrier dependent infectious diseases with environmental effects, *Nonlinear Anal. Modell. Control*, **13** (2008), 331–350. https://doi.org/10.15388/NA.2008.13.3.14561
8. P. K. Tiwari, R. K. Rai, S. Khajanchi, R. K. Gupta, A. K. Misra, Dynamics of coronavirus pandemic: effects of community awareness and global information campaigns, *Eur. Phys. J. Plus*, **136** (2021), 994. https://doi.org/10.1140/epjp/s13360-021-01997-6
9. J. Pang, J. A. Cui, J. Hui, Rich dynamics of epidemic model with sub-optimal immunity and nonlinear recovery rate, *Math. Comput. Modell.*, **54** (2011), 440–448. https://doi.org/10.1016/j.mcm.2011.02.033
10. C. T. Codeco, Endemic and epidemic dynamics of cholera: the role of the aquatic reservoir, *BMC Infect. Dis.*, **1** (2001), 1–14. https://doi.org/10.1186/1471-2334-1-1
11. M. E. Alexander, S. M. Moghadas, Periodicity in an epidemic model with a generalized non-linear incidence, *Math. Biosci.*, **189** (2004), 75–96. https://doi.org/10.1016/j.mbs.2004.01.003
12. J. K. Ghosh, S. K. Biswas, S. Sarkar, U. Ghosh, Mathematical modelling of COVID-19: A case study of Italy, *Math. Comput. Simul.*, **194** (2022), 1–18. https://doi.org/10.1016/j.matcom.2021.11.008
13. H. W. Hethcote, The mathematics of infectious diseases, *SIAM Rev.*, **42** (2000), 599–653. https://doi.org/10.1137/S0036144500371907
14. X. Meng, S. Zhao, T. Feng, T. Zhang, Dynamics of a novel nonlinear stochastic SIS epidemic model with double epidemic hypothesis, *J. Math. Anal. Appl.*, **433** (2016), 227–242. https://doi.org/10.1016/j.jmaa.2015.07.056
15. A. Rajput, M. Sajid, Tanvi, C. Shekhar, R. Aggarwal, Optimal control strategies on COVID-19 infection to bolster the efficacy of vaccination in India, *Sci. Rep.*, **11** (2021), 1–18. https://doi.org/10.1038/s41598-021-99088-0

16. B. Dhar, P. K. Gupta, M. Sajid, Solution of a dynamical memory effect COVID-19 infection system with leaky vaccination efficacy by non-singular kernel fractional derivatives, *Math. Biosci. Eng*, **19** (2022), 4341–4367. https://doi.org/10.3934/mbe.2022201

17. F. Bozkurt, A. Yousef, T. Abdeljawad, A. Kalinli, Q. Al Mdallal, A fractional-order model of COVID-19 considering the fear effect of the media and social networks on the community, *Chaos, Solitons Fractals*, **152** (2021), 111403. https://doi.org/10.1016/j.chaos.2021.111403

18. M. Asif, Z. A. Khan, N. Haider, Q. Al-Mdallal, Numerical simulation for solution of SEIR models by meshless and finite difference methods, *Chaos, Solitons Fractals*, **141** (2020), 110340. https://doi.org/10.1016/j.chaos.2020.110340

19. M. Umar, Kusen, M. A. Z. Raja, Z. Sabir, Q. Al-Mdallal, A computational framework to solve the nonlinear dengue fever SIR system, *Comput. Methods Biomech. Biomed. Eng.*, **2022** (2022), 1–14. https://doi.org/10.1080/10255842.2022.2039640

20. A. Abdelrazec, J. Bélair, C. Shan, H. Zhu, Modeling the spread and control of dengue with limited public health resources, *Math. Biosci.*, **271** (2016), 136–145. https://doi.org/10.1016/j.mbs.2015.11.004

21. R. Boaden, N. Proudlove, M. Wilson, An exploratory study of bed management, *J. Manage. Med.*, **13** (1999), 234–250. https://doi.org/10.1108/02689239910292945

22. R. D. Booton, L. MacGregor, L. Vass, K. J. Looker, C. Hyams, P. D. Bright, et al., Estimating the COVID-19 epidemic trajectory and hospital capacity requirements in South West England: a mathematical modelling framework, *BMJ Open*, **11** (2021), e041536. https://doi.org/10.1136/bmjopen-2020-041536

23. I. Area, X. H. Vidal, J. J. Nieto, M. J. P. Hermida, Determination in Galicia of the required beds at Intensive Care Units, *Alex. Eng. J.*, **60** (2021), 559–564. https://doi.org/10.1016/j.aej.2020.09.034

24. S. D. D. Njankou, F. Nyabadza, Modelling the potential impact of limited hospital beds on Ebola virus disease dynamics, *Math. Methods Appl. Sci.*, **41** (2018), 8528–8544. https://doi.org/10.1002/mma.4789

25. B. Dubey, A. Patra, P. K. Srivastava, U. S. Dubey, Modeling and analysis of an SEIR model with different types of nonlinear treatment rates, *J. Biol. Syst.*, **21** (2013), 1350023. https://doi.org/10.1142/S021833901350023X

26. L. V. Green, How many hospital beds, *INQUIRY: J. Health Care Organ. Provis. Financing*, **39** (2002), 400–412. https://doi.org/10.5034/inquiryjrnl_39.4.400

27. J. Karnon, M. Mackay, T. M. Mills, Mathematical modelling in health care, in *18th World IMACS/MODSIM Congress*, (2009), 44–56. https://doi.org/10.1.1.552.4422

28. A. Kumar, P. K. Srivastava, R. P. Gupta, Nonlinear dynamics of infectious diseases via information-induced vaccination and saturated treatment, *Math. Comput. Simul.*, **157** (2019), 77–99. https://doi.org/10.1016/j.matcom.2018.09.024

29. A. K. Misra, J. Maurya, Modeling the importance of temporary hospital beds on the dynamics of emerged infectious disease, *Chaos Interdiscip. J. Nonlinear Sci.*, **31** (2021), 103125. https://doi.org/10.1063/5.0064732

30. W. Qin, S. Tang, C. Xiang, Y. Yang, Effects of limited medical resource on a Filippov infectious disease model induced by selection pressure, *Appl. Math. Comput.*, **283** (2016), 339–354. https://doi.org/10.1016/j.amc.2016.02.042
31. P. Saha, U. Ghosh, Global dynamics and control strategies of an epidemic model having logistic growth, non-monotone incidence with the impact of limited hospital beds, *Nonlinear Dyn.*, **105** (2021), 971–996. https://doi.org/10.1007/s11071-021-06607-9
32. C. Shan, H. Zhu, Bifurcations and complex dynamics of an SIR model with the impact of the number of hospital beds, *J. Differ. Equations*, **257** (2014), 1662–1688. https://doi.org/10.1016/j.jde.2014.05.030
33. C. Shan, Y. Yi, H. Zhu, Nilpotent singularities and dynamics in an SIR type of compartmental model with hospital resources, *J. Differ. Equations*, **260** (2016), 4339–4365. https://doi.org/10.1016/j.jde.2015.11.009
34. A. Wang, Y. Xiao, H. Zhu, Dynamics of a Filippov epidemic model with limited hospital beds, *Math. Biosci. Eng.*, **15** (2018), 739. https://doi.org/10.3934/mbe.2018033
35. M. Zhang, J. Ge, Z. Lin, The impact of the number of hospital beds and spatial heterogeneity on an SIS epidemic model, *Acta Appl. Math.*, **167** (2020), 59–73. https://doi.org/10.1007/s10440-019-00268-y
36. X. Zhang, X. Liu, Backward bifurcation and global dynamics of an SIS epidemic model with general incidence rate and treatment, *Nonlinear Anal. Real World Appl.*, **10** (2009), 565–575. https://doi.org/10.1016/j.nonrwa.2007.10.011
37. H. Zhao, L. Wang, S. M. Oliva, H. Zhu, Modeling and dynamics analysis of Zika transmission with limited medical resources, *Bull. Math. Biol.*, **82** (2020), 1–50. https://doi.org/10.1007/s11538-020-00776-1
38. M. Zhu, Z. Lin, Modeling the transmission of dengue fever with limited medical resources and self-protection, *Discrete Contin. Dyn. Syst. B*, **23** (2018), 957. https://doi.org/10.3934/dcdsb.2018050
39. C. Castillo-Chavez, B. Song, Dynamical models of tuberculosis and their applications, *Math. Biosci. Eng.*, **1** (2004), 361. https://10.3934/mbe.2004.1.361
40. B. Dubey, A. Kumar, Stability switching and chaos in a multiple delayed prey–predator model with fear effect and anti-predator behavior, *Math. Comput. Simul.*, **188** (2021), 164–192. https://doi.org/10.1016/j.matcom.2021.03.037
41. H. L. Freedman, V. S. H. Rao, The trade-off between mutual interference and time lags in predator-prey systems, *Bull. Math. Biol.*, **45** (1983), 991–1004. https://doi.org/10.1016/S0092-8240(83)80073-1
42. K. Gopalsamy, *Stability and Oscillations in Delay Differential Equations of Population Dynamics*, Springer Science & Business Media, 2013.